

Combating Confirmation Bias: A Unified Pseudo-Labeling Framework for Entity Alignment

Qijie Ding¹, Jie Yin^{1*}, Daokun Zhang², Junbin Gao¹

¹Discipline of Business Analytics, The University of Sydney, Sydney, NSW, Australia.

²Department of Data Science & AI, Monash University, Melbourne, VIC, Australia.

*Corresponding author(s). E-mail(s): jie.yin@sydney.edu.au;

Contributing authors: qijie.ding@sydney.edu.au;

daokun.zhang@monash.edu; junbin.gao@sydney.edu.au;

Abstract

Entity alignment (EA) aims at identifying equivalent entity pairs across different knowledge graphs (KGs) that refer to the same real-world identity. It has been a compelling but challenging task that requires the integration of heterogeneous information from different KGs to expand the knowledge coverage and enhance inference abilities. To circumvent the shortage of prior seed alignments provided for training, recent EA models utilize pseudo-labeling strategies to iteratively add unaligned entity pairs predicted with high confidence to the prior seed alignments for model retraining. However, the adverse impact of confirmation bias during pseudo-labeling has been largely overlooked, thus hindering entity alignment performance. To systematically combat confirmation bias, we propose a new Unified Pseudo-Labeling framework for Entity Alignment (UPL-EA) that explicitly alleviates pseudo-labeling errors to boost the performance of entity alignment. UPL-EA achieves this goal through two key innovations: (1) Optimal Transport (OT)-based pseudo-labeling uses discrete OT modeling as an effective means to determine entity correspondences and reduce erroneous matches across two KGs. An effective criterion is derived to infer pseudo-labeled alignments that satisfy one-to-one correspondences at each iteration; (2) Pseudo-label ensembling refines pseudo-labeled alignments by combining predictions over multiple pseudo-labeling iterations. The refined pseudo-labeled alignments are thereafter used to augment prior seed alignments to reinforce subsequent model training for alignment inference. The effectiveness of UPL-EA in eliminating pseudo-labeling errors is both theoretically supported and experimentally validated. Our extensive results and in-depth analyses demonstrate the superiority of UPL-EA over

15 competitive baselines and its utility as a general pseudo-labeling framework for entity alignment.

Keywords: Entity Alignment, Pseudo-labeling, Optimal Transport, Knowledge Graphs

1 Introduction

Knowledge Graphs (KGs) are large-scale structured knowledge bases that represent real-world entities (or concepts) and their relationships as a collection of factual triplets. Recent years have witnessed the release of various open-source KGs (e.g., Freebase (Bollacker et al, 2008), YAGO (Suchanek et al, 2007) and Wikidata (Vrandečić and Krötzsch, 2014)) from general to specific domains and their proliferation to empower many artificial intelligence (AI) applications, such as recommender systems (Guo et al, 2022), question answering (Yang et al, 2018) and information retrieval (Paulheim, 2017). Nevertheless, it has become a well-known fact that real-world KGs suffer from incompleteness arising from their complex, semi-automatic construction process. This has led to an increasing number of research efforts on KG completion, such as TransE (Bordes et al, 2013) and TransH (Wang et al, 2014), which aim to add missing facts to individual KGs. Unfortunately, due to its limited coverage and incompleteness, a single KG cannot fulfill the requirements for complex AI applications that build upon heterogeneous knowledge sources. This necessitates the integration of heterogeneous information from multiple individual KGs to enrich knowledge representation. Entity alignment (EA) is a crucial task towards this objective, which aims to establish the correspondence between equivalent entity pairs across different KGs that refer to the same real-world identity.

Over the last decade, there has been a surge of research efforts dedicated to entity alignment across KGs. Most mainstream EA models are embedding-based; they embed KGs into a shared latent embedding space so that similarities between entities can be measured via their embeddings for alignment inference. To leverage structural information in KGs, more recent EA models exploit the power of Graph Neural Networks (GNNs) to encode KG structures for entity alignment. Methods like GCN-Align Wang et al (2018) utilize GCNs to learn better entity embeddings by aggregating features from neighboring entities. However, GCNs and their variants suffer from an over-smoothing issue (Min et al, 2020; Jiang et al, 2022), where the embeddings of entities among local neighborhoods become indistinguishably similar as the number of convolution layers increases. To alleviate over-smoothing during GCN neighborhood aggregation, recent works Wu et al (2019b,a); Zhu et al (2021) use a highway strategy Srivastava et al (2015) on GCN layers, which “mixes” the smoothed entity embeddings with the original features. Despite achieving competitive results, these methods require an abundant amount of pre-aligned entity pairs (known as *prior seed alignments*) provided for training, which are labor-intensive and costly to acquire in real-world KGs. To tackle the shortage of prior seed alignments, recently proposed models, such as BootEA (Sun et al, 2018), IPTransE (Zhu

et al, 2017), MRAEA (Mao et al, 2020), and RNM (Zhu et al, 2021), adopt a bootstrapping strategy that iteratively selects unaligned entity pairs predicted with high confidence as pseudo-labeled alignments and adds them to prior seed alignments for model retraining. The bootstrapping strategy, originating from the field of statistics, is also referred to as pseudo-labeling—a predominant learning paradigm proposed to tackle label scarcity in semi-supervised learning.

In general semi-supervised learning, pseudo-labeling approaches inherently suffer from confirmation bias (Arazo et al, 2020; Tarvainen and Valpola, 2017). The confirmation bias refers to using incorrectly predicted labels generated on unlabeled data for subsequent training, thereby misleadingly increasing model confidence in incorrect predictions and leading to a biased model with degraded performance. Unfortunately, there is a lack of understanding of the fundamental factors that give rise to confirmation bias for pseudo-labeling-based entity alignment. Our analysis (see Section 2.2) advocates that the confirmation bias is exacerbated during pseudo-labeling for entity alignment. Due to the lack of sufficient prior seed alignments at the early stages of training, the existing models tend to learn uninformative entity embeddings and consequently generate error-prone pseudo-labeled alignments based on unreliable model predictions. We characterize pseudo-labeling errors into two types: (1) **Type I pseudo-labeling errors** refer to *conflicted misalignments*, where a single entity in one KG is simultaneously aligned with multiple entities in another KG with erroneous matches. (2) **Type II pseudo-labeling errors** refer to *one-to-one misalignments*, where an entity in one KG is incorrectly matched with an entity in another KG. The pseudo-labeling errors, if not properly mitigated, would propagate into subsequent model training, thereby jeopardizing the efficacy of pseudo-labeling-based entity alignment. However, current pseudo-labeling-based EA models have made only limited attempts to alleviate alignment conflicts using simple heuristics (Zhu et al, 2017; Sun et al, 2019; Mao et al, 2020; Zhu et al, 2021) or imposing constraints to enforce hard alignments (Sun et al, 2018; Ding et al, 2022), while the confirmation bias has been left under-explored.

To address the research gap, we propose a novel unified pseudo-labeling framework for entity alignment (UPL-EA) aimed at alleviating confirmation bias and improving entity alignment performance. The key idea lies in “reliably” pseudo-labeling unaligned entity pairs based on model predictions and augmenting prior seed alignments to iteratively improve model performance. UPL-EA comprises two essential components: Optimal Transport (OT)-based pseudo-labeling and pseudo-label ensembling, to effectively reduce pseudo-labeling errors. OT-based pseudo-labeling considers entity alignment as a probabilistic matching process between entity sets in two KGs. An effective criterion is mathematically derived to select pseudo-labeled alignments that satisfy one-to-one correspondences, thus mitigating conflicted misalignments (Type I pseudo-labeling errors) at each iteration. Pseudo-label ensembling reduces the pseudo-label selection variability by finding consensus predictions over multiple pseudo-labeling iterations, thereby eliminating one-to-one misalignments (Type II pseudo-labeling errors). The refined pseudo-labeled alignments are used to augment prior seed alignments to reinforce subsequent model training for alignment inference. To our best knowledge, we are the first to address the confirmation bias inherent

in pseudo-labeling-based entity alignment. Comprehensive experiments and analyses validate the superior performance of UPL-EA over state-of-the-art supervised and semi-supervised baselines and its utility as a general pseudo-labeling framework to improve entity alignment performance.

The remainder of this paper is organized as follows. Section 2 provides a problem statement of pseudo-labeling-based entity alignment and presents an empirical analysis of confirmation bias that motivates this work. Section 3 presents the proposed framework, followed by an in-depth experimental evaluation reported in Section 4. Related works are discussed in Section 5, and we conclude the paper in Section 6.

2 Preliminaries

In this section, we first provide a problem statement of pseudo-labeling-based entity alignment. Then, we perform a thorough analysis of confirmation bias during pseudo-labeling, which motivates the design of our proposed framework.

2.1 Problem Statement

A knowledge graph (KG) can be represented as $\mathcal{G} = \{\mathcal{E}, \mathcal{R}, \mathcal{T}\}$ with the entity set \mathcal{E} , relation set \mathcal{R} , and relational triplet set \mathcal{T} . Each triplet is denoted as $(e_i, r, e_j) \in \mathcal{T}$, which represents that a head entity $e_i \in \mathcal{E}$ is connected to a tail entity $e_j \in \mathcal{E}$ via a relation $r \in \mathcal{R}$. Each entity e_i is characterized by an entity feature vector $\mathbf{x}_i \in \mathbb{R}^f$, which can be obtained from entity names with semantic meanings.

Formally, given two KGs, $\mathcal{G}_1 = \{\mathcal{E}_1, \mathcal{R}_1, \mathcal{T}_1\}$ and $\mathcal{G}_2 = \{\mathcal{E}_2, \mathcal{R}_2, \mathcal{T}_2\}$, the task of entity alignment (EA) aims to discover a set of one-to-one equivalent entity pairs $\mathcal{I} = \{(e_i, e_j) \in \mathcal{E}_1 \times \mathcal{E}_2 \mid e_i \equiv e_j\}$ between \mathcal{G}_1 and \mathcal{G}_2 , where $e_1 \in \mathcal{E}_1$, $e_2 \in \mathcal{E}_2$, and \equiv indicates an equivalence relationship between e_1 and e_2 . In many cases, a small set of equivalent entity pairs $\mathcal{S}_0 \in \mathcal{I}$, known as prior seed alignments, is provided beforehand and used as training data. Apart from entities included in \mathcal{S}_0 , there are two sets of unaligned entities $\mathcal{E}_1^U \subset \mathcal{E}_1$ and $\mathcal{E}_2^U \subset \mathcal{E}_2$ in \mathcal{G}_1 and \mathcal{G}_2 , respectively.

In this work, we consider real-world scenarios where prior seed alignments \mathcal{S}_0 are usually scarce due to high labeling costs. We focus on the task of pseudo-labeling-based entity alignment, which aims to leverage both prior seed alignments and unaligned entity pairs to more effectively train an EA model in semi-supervised settings. This is achieved by iteratively selecting a set of unaligned entity pairs as pseudo-labeled alignments $\hat{\mathcal{S}} \subset \mathcal{E}_1^U \times \mathcal{E}_2^U$ and using $\hat{\mathcal{S}}$ to augment prior seed alignments \mathcal{S}_0 , i.e., $\mathcal{S}_0 \leftarrow \mathcal{S}_0 \cup \hat{\mathcal{S}}$, for subsequent model retraining.

2.2 Analysis of Confirmation Bias

The key to pseudo-labeling-based entity alignment lies in selecting reliable pseudo-labeled alignments to effectively boost model performance; otherwise, pseudo-labeling errors could propagate into subsequent model training, leading to confirmation bias (Araza et al, 2020). To investigate the impact of confirmation bias on pseudo-labeling-based entity alignment, we perform an error analysis of a naive pseudo-labeling strategy used in previous studies (Sum et al, 2019). This strategy simply

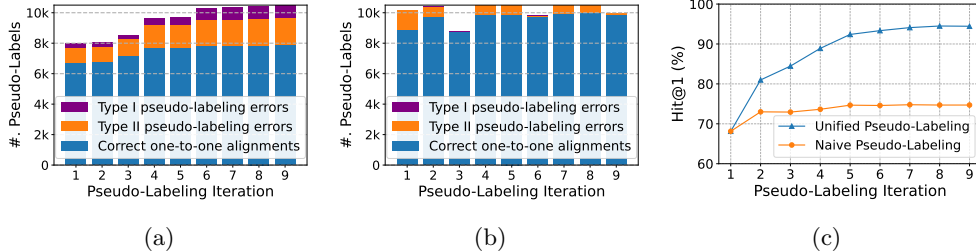


Fig. 1: Error analysis of confirmation bias. (a) Number of pseudo-labeled alignments selected by a naive pseudo-labeling strategy over pseudo-labeling iterations. (b) Number of pseudo-labeled alignments selected by the proposed UPL strategy over pseudo-labeling iterations. (c) Entity alignment performance comparison (Hit@1) of the naive pseudo-labeling strategy and the proposed UPL strategy.

selects pairs of unaligned entities whose embedding distances (defined using Eq. (6)) are smaller than a pre-specified threshold as pseudo-labeled alignments. Our analysis is carried out on a widely used cross-lingual KG pair, DBP15K_{ZH,EN} (with details presented in Section 4.1), using the conventional 30%-70% split ratio to randomly partition the 15,000 ground truth entity alignments into training and test data. To understand the underlying causes of confirmation bias, we explicitly calculate the numbers of Type I and Type II pseudo-labeling errors, along with the number of correctly pseudo-labeled alignments, at different pseudo-labeling iterations on the test data.

As shown in Fig. 1a, the naive pseudo-labeling strategy selects only a relatively small number of correctly pseudo-labeled alignments in the first three iterations (although Type I and Type II pseudo-labeling errors seem low). Thus, the corresponding performance in Fig. 1c shows minimal improvements. From the fourth iteration, although the number of correctly pseudo-labeled alignments gradually increases, Type I and Type II pseudo-labeling errors also propagate and increase as the training proceeds. This accumulation of errors give rise to confirmation bias, severely hindering the capability of pseudo-labeling for performance improvements.

Our analysis affirms that the confirmation bias essentially stems from Type I and Type II pseudo-labeling errors. These errors, if not adequately addressed, would propagate into subsequent model training, thus diminishing the effectiveness of pseudo-labeling for entity alignment. Our work is thus motivated to explicitly eliminate Type I and Type II pseudo-labeling errors. As evidenced in Fig. 1b, our proposed Unified Pseudo-Labeling (UPL) strategy effectively eliminates all Type I pseudo-labeling errors across all iterations while mitigating the number of Type II pseudo-labeling errors, leading to substantial performance gains as shown in Fig. 1c.

3 The Proposed UPL-EA Framework

With insights from our analysis in Section 2.2, the proposed UPL-EA framework is designed to systematically address confirmation bias for pseudo-labeling-based entity alignment. The core of UPL-EA is a new Unified Pseudo-Labeling (UPL) strategy

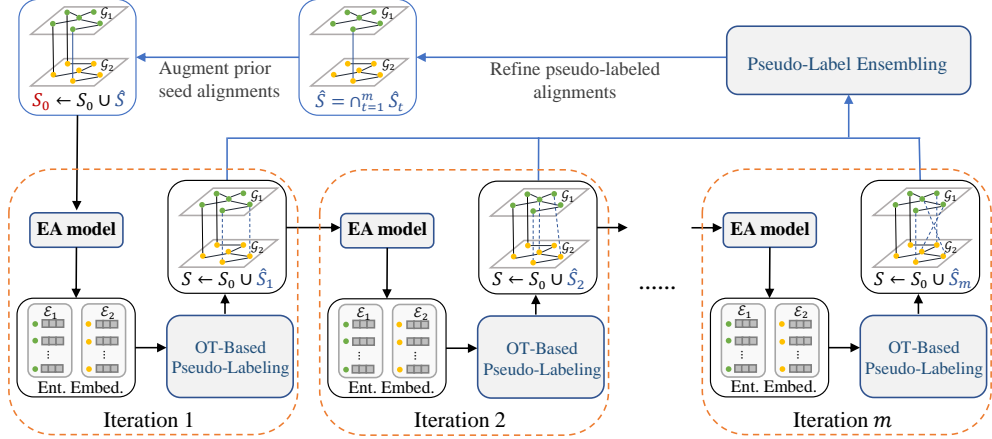


Fig. 2: An overview of the proposed UPL-EA framework.

that iteratively generates reliable pseudo-labeled alignments to enhance the entity alignment (EA) model. UPL utilizes two essential components: (1) OT-based pseudo-labeling, which generates pseudo-labeled alignments with one-to-one correspondences, effectively eliminating conflicted misalignments at each iteration (**Addressing Type I pseudo-labeling errors**); and (2) pseudo-label ensembling, which combines pseudo-labeled alignments generated through OT modeling over multiple iterations, reducing prediction variability and mitigating one-to-one misalignments across iterations (**Addressing Type II pseudo-labeling errors**).

Fig. 2 illustrates an overview of the proposed UPL-EA framework. At each iteration t , the EA model learns entity embeddings based on the available seed alignments \mathcal{S} . OT-Based Pseudo-Labeling then takes entity embeddings as input to generate pseudo-labeled alignments $\hat{\mathcal{S}}_t$, which are combined with prior seed alignments \mathcal{S}_0 to train the EA model in the next iteration $t + 1$. After every m iterations, pseudo-labeled alignments generated over multiple iterations $\{\hat{\mathcal{S}}_t | t = 1, \dots, m\}$ are passed on to Pseudo-Label Ensembling for further refinement, preventing one-to-one misalignments from propagating into subsequent model training. The refined pseudo-labeled alignments $\hat{\mathcal{S}}$ are used to augment prior seed alignments \mathcal{S}_0 , i.e., $\mathcal{S}_0 \leftarrow \mathcal{S}_0 \cup \hat{\mathcal{S}}$, which are subsequently used in the next m iterations for model training. The EA model and the UPL strategy mutually reinforce each other to learn informative entity embeddings. Lastly, the learned entity embeddings are used for entity alignment inference.

3.1 Entity Alignment Model

The entity alignment (EA) model aims to learn informative entity embeddings and perform model training for entity alignment inference. Our UPL-EA framework is designed to be modular, allowing for the use of various existing EA models. In this work, we present one instantiation based on our previous work (Ding et al, 2022).

3.1.1 Entity Embedding

To enable the EA model to learn informative entity embeddings, it is essential to capture structural information inherent in KGs. In this work, we employ a global-local neighborhood aggregation scheme (Ding et al, 2022) that has the advantages of encoding both global and local patterns in KG structures.

Global-Level Relation Aggregation. To capture the global patterns of a given relation r , we construct its feature vector \mathbf{x}_r by considering all triplets associated with r in two KGs. Specifically, for each relation $r \in \mathcal{R}_1 \cup \mathcal{R}_2$, we compute its feature vector \mathbf{x}_r by averaging the concatenated feature vectors of its corresponding head and tail entities:

$$\mathbf{x}_r = \text{Average}(\{[\mathbf{x}_i \parallel \mathbf{x}_j] \mid (e_i, r, e_j) \in \mathcal{T}_1 \cup \mathcal{T}_2\}), \quad (1)$$

where $[\cdot \parallel \cdot]$ denotes the concatenation operation, \mathbf{x}_i and $\mathbf{x}_j \in \mathbb{R}^f$ are the feature vectors of entity e_i and e_j , respectively. The resulting feature vector $\mathbf{x}_r \in \mathbb{R}^{2f}$ can capture the intrinsic relational semantics of relation r . Next, for each entity $e_i \in \mathcal{E}_1 \cup \mathcal{E}_2$, we construct its aggregated neighboring relation feature as follows:

$$\mathbf{x}_i^{\text{rel}} = \text{Average}(\{\mathbf{x}_r \mid r \in \mathcal{N}_r(e_i)\}), \quad (2)$$

where $\mathcal{N}_r(e_i)$ is the set of one-hop neighboring relations of entity e_i .

To perform global-level relation aggregation, we concatenate each entity’s averaged neighboring relation feature $\mathbf{x}_i^{\text{rel}} \in \mathbb{R}^{2f}$ with its original feature $\mathbf{x}_i \in \mathbb{R}^f$, followed by a non-linear transformation. To avoid over-smoothing, the original entity feature vector $\mathbf{x}_i \in \mathbb{R}^f$ is also added via a residual connection. The relation aggregated entity embedding is obtained as:

$$\mathbf{h}_i^{(1)} = \text{ReLU}(\mathbf{W}[\mathbf{x}_i \parallel \mathbf{x}_i^{\text{rel}}] + \mathbf{b}) + \mathbf{x}_i, \quad (3)$$

where $\mathbf{h}_i^{(1)} \in \mathbb{R}^d$ and d is the dimension of entity embedding. $\mathbf{W} \in \mathbb{R}^{d \times 3f}$ and $\mathbf{b} \in \mathbb{R}^d$ are learnable parameters. Generally, the dimensions of entity embedding and entity feature are different. Here, for the residual connection, we set $d = f$.

Local-Level Entity Aggregation. After obtaining entity embeddings via relation aggregation at the global level, we further perform local-level entity aggregation to capture neighboring entity structures. For this purpose, we employ a two-layer GCN connected by a highway gate strategy (Srivastava et al, 2015) to avoid over-smoothing. Formally, the entity embedding vector $\mathbf{h}_i^{(1)}$ is updated as follows:

$$\mathbf{h}_i^{(l+1)} = \text{Aggregate}(\{\mathbf{h}_j^{(l)} \mid e_j \in \mathcal{N}_e(e_i) \cup \{e_i\}\}), \quad (4)$$

where $\mathcal{N}_e(e_i)$ is the set of one-hop neighboring entities of entity e_i , $\text{Aggregate}(\cdot)$ denotes the aggregation function specific to a high-way GCN encoder. Finally, the embedding for entity e_i is obtained as $\mathbf{h}_i = \mathbf{h}_i^{(3)} \in \mathbb{R}^d$.

3.1.2 Model Training for Embedding Learning

Given a set of seed alignments \mathcal{S} , we define a margin-based loss function for embedding learning, such that the equivalent entities are encouraged to be close to each other in the embedding space:

$$L = \sum_{(e_i, e_j) \in \mathcal{S}} \sum_{(e_i^-, e_j^-) \in \mathcal{S}_{(e_i, e_j)}^-} \max(0, d(e_i, e_j) - d(e_i^-, e_j^-) + \gamma), \quad (5)$$

where $\mathcal{S}_{(e_i, e_j)}^- = \{(e_i, e_j^-) \mid e_j^- \in \mathcal{E}_2 \setminus \{e_j\}\} \cup \{(e_i^-, e_j) \mid e_i^- \in \mathcal{E}_1 \setminus \{e_i\}\}$ denotes the set of negative alignments, synthesized by negative sampling of a positive alignment $(e_i, e_j) \in \mathcal{S}$ as $(e_i, e_j^-) \notin \mathcal{S}$ and $(e_i^-, e_j) \notin \mathcal{S}$. γ is a hyper-parameter that determines the margin to separate positive alignments from negative alignments. $d(e_i, e_j)$ indicates the embedding distance between entity pair (e_i, e_j) across two KGs, defined as:

$$d(e_i, e_j) = \|\mathbf{h}_i - \mathbf{h}_j\|_1. \quad (6)$$

The loss function in Eq. (5) can be minimized with respect to entity embeddings $\{\mathbf{h}_i \mid e_i \in \mathcal{E}_1 \cup \mathcal{E}_2\}$. To facilitate model training, we adopt an *adaptive negative sampling* strategy to obtain the set of negative alignments $\mathcal{S}_{(e_i, e_j)}^-$. Specifically, for each positive alignment $(e_i, e_j) \in \mathcal{S}$, we select K nearest entities of e_i (or e_j), measured using the embedding distance in Eq. (6), to replace e_j (or e_i) and form K negative counterparts (e_i, e_j^-) (or (e_i^-, e_j)). This adaptive strategy helps generate “hard” negative alignments and push their associated entities to be apart from each other in the embedding space.

3.2 Unified Pseudo-Labeling Strategy

After training the EA model, the learned entity embeddings can be used for alignment inference. However, as prior seed alignments provided for training are often limited, the performance of entity alignment can be suboptimal. Therefore, pseudo-labeling strategies can be designed to select a set of unaligned entity pairs as pseudo-labeled alignments, which are used to augment prior seed alignments for boost model training. However, as discussed in Section 2.2, a naive strategy might introduce a large number of pseudo-labeling errors, leading to confirmation bias. To address this, we propose the Unified Pseudo-Labeling (UPL) that explicitly aims to mitigate Type I and Type II pseudo-labeling errors.

In what follows, the two essential components of UPL: OT-based pseudo-labeling and pseudo-label ensembling, are discussed in detail.

3.2.1 OT-Based Pseudo-Labeling

To mitigate Type I pseudo-labeling errors, we propose using Optimal Transport (OT) as an effective means to reliably pseudo-label unaligned entities across KGs to reinforce the training of the EA model. As a powerful mathematical framework for transforming one distribution into another, OT allows us to more effectively identify one-to-one correspondences between entities, ensuring a coherent alignment configuration.

Formally, we model the alignment between two unaligned entity sets \mathcal{E}_1^U and \mathcal{E}_2^U as an OT process to warrant one-to-one alignments, i.e., transporting each entity $e_i \in \mathcal{E}_1^U$ to a unique entity $e_j \in \mathcal{E}_2^U$, with minimal overall transport cost. Denote $\mathbf{C} \in \mathbb{R}^{|\mathcal{E}_1^U| \times |\mathcal{E}_2^U|}$ as the transport cost matrix, and without loss of generality, we assume $|\mathcal{E}_1^U| < |\mathcal{E}_2^U|$. The transport plan is a mapping function $T : e_i \rightarrow T(e_j)$, where $e_i \in \mathcal{E}_1^U$, $T(e_i) \in \mathcal{E}_2^U$. Thus, the objective of entity alignment is to find the optimal transport plan T^* that minimizes the overall transport cost:

$$T^* = \arg \min_T \sum_{e_i \in \mathcal{E}_1^U} \mathbf{C}_{e_i, T(e_i)}. \quad (7)$$

A critical aspect of the above objective is defining a reliable measure of the transport cost. One might directly use the distances between the learned entity embeddings. However, when only a limited set of prior seed alignments are available for training, the learned entity embeddings can be uninformative, particularly during the early training stages before the EA model has converged. As a result, using these embeddings to calculate the distances for defining the transport cost can be error-prone. To address this, we resort to rectifying the embedding distance using relational neighborhood matching (Zhu et al, 2021), which complements the training of the EA model, especially during the early stages, for learning better entity embeddings and providing a more reliable cost measure for OT modeling. The principle of distance rectification is to leverage relational contexts within local neighborhoods to help determine the extent to which two entities should be aligned. Intuitively, if two entities $e_i \in \mathcal{E}_1$ and $e_j \in \mathcal{E}_2$ share more aligned neighboring entities/relations, the distance between their embeddings should be smaller, indicating a higher likelihood of being aligned to each other. Based on this intuition, the transport cost for OT-based pseudo-labeling is defined as follows:

$$\mathbf{C}_{e_i, e_j} = d(e_i, e_j) - \lambda s(e_i, e_j), \quad e_i \in \mathcal{E}_1^U, e_j \in \mathcal{E}_2^U, \quad (8)$$

where λ is a trade-off hyper-parameter, and $s(e_i, e_j)$ is a scoring function indicating the degree to which the relational contexts of two entities e_i and e_j match. Let $\mathcal{M}_{(e_i, e_j)}$ represent the set of aligned neighboring relation-entity tuples for entity pair (e_i, e_j) , obtained following (Zhu et al, 2021). The score $s(e_i, e_j)$ is calculated as:

$$s(e_i, e_j) = \frac{\sum_{(r, e_k) \in \mathcal{M}_{(e_i, e_j)}} P_1(r, e_k) P_2(r, e_k)}{|\mathcal{N}_e(e_i)| + |\mathcal{N}_e(e_j)|}, \quad (9)$$

where $\mathcal{N}_e(e_i)$ and $\mathcal{N}_e(e_j)$ denote the sets of neighboring entities for e_i and e_j , respectively. $P_1(r, e_k)$ and $P_2(r, e_k)$ indicate the reciprocal frequency of triplets associated with neighboring tuple (r, e_k) for e_i in \mathcal{T}_1 and e_j in \mathcal{T}_2 , respectively.

The objective in Eq. (7) defines a hard assignment optimization problem, which, however, does not scale well. To enable more efficient optimization and to allow for a more flexible alignment configuration, we reformulate this objective as a discrete OT problem, where the optimal transport plan is considered as a coupling matrix

$\mathbf{P}^* \in \mathbb{R}_+^{|\mathcal{E}_1^U| \times |\mathcal{E}_2^U|}$ between two discrete distributions. Denote $\boldsymbol{\mu}$ and $\boldsymbol{\nu}$ as two discrete probability distributions over all entities $\{e_i | e_i \in \mathcal{E}_1^U\}$ and $\{e_j | e_j \in \mathcal{E}_2^U\}$, respectively. Without any alignment preference, the two discrete distributions $\boldsymbol{\mu}$ and $\boldsymbol{\nu}$ are assumed to follow a uniform distribution such that $\boldsymbol{\mu} = \frac{1}{|\mathcal{E}_1^U|} \sum_{e_i \in \mathcal{E}_1^U} \delta_{e_i}$ and $\boldsymbol{\nu} = \frac{1}{|\mathcal{E}_2^U|} \sum_{e_j \in \mathcal{E}_2^U} \delta_{e_j}$, where δ_{e_i} and δ_{e_j} are the Dirac function centered on e_i and e_j , respectively. Both $\boldsymbol{\mu}$ and $\boldsymbol{\nu}$ are bounded to sum up to one: $\sum_{e_i \in \mathcal{E}_1^U} \boldsymbol{\mu}(e_i) = \sum_{e_i \in \mathcal{E}_1^U} \frac{1}{|\mathcal{E}_1^U|} = 1$ and $\sum_{e_j \in \mathcal{E}_2^U} \boldsymbol{\nu}(e_j) = \sum_{e_j \in \mathcal{E}_2^U} \frac{1}{|\mathcal{E}_2^U|} = 1$. Accordingly, the OT objective is formulated to find the optimal coupling matrix \mathbf{P}^* between $\boldsymbol{\mu}$ and $\boldsymbol{\nu}$:

$$\begin{aligned} \mathbf{P}^* &= \arg \min_{\mathbf{P} \in \Pi(\boldsymbol{\mu}, \boldsymbol{\nu})} \sum_{e_i \in \mathcal{E}_1^U} \sum_{e_j \in \mathcal{E}_2^U} \mathbf{P}_{e_i, e_j} \cdot \mathbf{C}_{e_i, e_j}, & (10) \\ \text{subject to: } & \sum_{e_j \in \mathcal{E}_2^U} \mathbf{P}_{e_i, e_j} = \boldsymbol{\mu}(e_i) = \frac{1}{|\mathcal{E}_1^U|}, \\ & \sum_{e_i \in \mathcal{E}_1^U} \mathbf{P}_{e_i, e_j} = \boldsymbol{\nu}(e_j) = \frac{1}{|\mathcal{E}_2^U|}, \\ & \mathbf{P}_{e_i, e_j} \geq 0, \forall e_i \in \mathcal{E}_1^U, \forall e_j \in \mathcal{E}_2^U, \end{aligned}$$

where $\Pi(\boldsymbol{\mu}, \boldsymbol{\nu}) = \{\mathbf{P} \in \mathbb{R}_+^{|\mathcal{E}_1^U| \times |\mathcal{E}_2^U|} | \mathbf{P} \mathbf{1}_{|\mathcal{E}_2^U|} = \boldsymbol{\mu}, \mathbf{P}^\top \mathbf{1}_{|\mathcal{E}_1^U|} = \boldsymbol{\nu}\}$ is the set of all joint probability distributions with marginal probabilities $\boldsymbol{\mu}$ and $\boldsymbol{\nu}$, $\mathbf{1}_n$ denotes an n -dimensional vector of ones. \mathbf{P} is a coupling matrix signifying probabilistic alignments between two unaligned entity sets \mathcal{E}_1^U and \mathcal{E}_2^U . Therefore, \mathbf{P}_{e_i, e_j} indicates the amount of probability mass transported from $\boldsymbol{\mu}(e_i)$ to $\boldsymbol{\nu}(e_j)$. A larger value of \mathbf{P}_{e_i, e_j} indicates a higher likelihood of e_i and e_j being aligned to each other.

To solve the discrete OT problem in Eq. (10), several exact algorithms have been proposed, such as interior point methods (Wächter and Biegler, 2006) and network simplex (Orlin, 1997). While these exact algorithms guarantee to find a closed-form optimal transport plan, their high computational cost makes them intractable for iterative pseudo-labeling. Thus, we propose to use an entropy regularized OT problem, as defined in Eq. (11) below, which can be solved by the efficient Sinkhorn algorithm (Cuturi, 2013).

$$\mathbf{P}^* = \arg \min_{\mathbf{P} \in \Pi(\boldsymbol{\mu}, \boldsymbol{\nu})} \sum_{e_i \in \mathcal{E}_1^U} \sum_{e_j \in \mathcal{E}_2^U} \mathbf{P}_{e_i, e_j} \cdot \mathbf{C}_{e_i, e_j} + \beta \sum_{e_i \in \mathcal{E}_1^U} \sum_{e_j \in \mathcal{E}_2^U} \mathbf{P}_{e_i, e_j} \log \mathbf{P}_{e_i, e_j}, \quad (11)$$

where β is a hyper-parameter that controls the strength of regularization. Solving the above entropy regularized OT problem can be easily implemented using popular deep-learning frameworks such as PyTorch and TensorFlow.

Once the optimal coupling matrix \mathbf{P}^* is estimated, entity alignments can be inferred accordingly. Since one-to-one correspondences are crucial for eliminating conflicted misalignments (Type I pseudo-labeling errors), we further propose a selection

criterion to identify entity pairs as pseudo-labeled alignments:

$$\widehat{\mathcal{S}}_t = \{(e_i, e_j) \mid \mathbf{P}_{e_i, e_j}^* > \frac{1}{2 \cdot \min(|\mathcal{E}_1^U|, |\mathcal{E}_2^U|)}, e_i \in \mathcal{E}_1^U, e_j \in \mathcal{E}_2^U\}. \quad (12)$$

This criterion ensures that the selected pseudo-labeled alignments satisfy one-to-one correspondence with theoretical guarantees. Unlike in previous works (Zhu et al, 2017; Sun et al, 2019; Mao et al, 2020; Zhu et al, 2021; Ding et al, 2022), this approach does not require pre-specifying the threshold.

Theorem 1. *Any pseudo-labeled alignment $(e_i, e_j), e_i \in \mathcal{E}_1^U, e_j \in \mathcal{E}_2^U$ that satisfies the condition $\mathbf{P}_{e_i, e_j}^* > \frac{1}{2 \cdot \min(|\mathcal{E}_1^U|, |\mathcal{E}_2^U|)}$ warrants one-to-one correspondence, such that no conflicted entity pairs, $\{(e_i, e_k) \mid e_k \in \mathcal{E}_2^U \setminus \{e_j\}\}$ and $\{(e_l, e_j) \mid e_l \in \mathcal{E}_1^U \setminus \{e_i\}\}$, are selected as pseudo-labeled alignments.*

Proof. Given the optimized coupling matrix $\mathbf{P}^* \in \mathbb{R}_+^{|\mathcal{E}_1^U| \times |\mathcal{E}_2^U|}$ subject to the constraints of $\sum_{e_j \in \mathcal{E}_2^U} \mathbf{P}_{e_i, e_j}^* = \frac{1}{|\mathcal{E}_1^U|}$ for all rows ($\forall e_i \in \mathcal{E}_1^U$) and $\sum_{e_i \in \mathcal{E}_1^U} \mathbf{P}_{e_i, e_j}^* = \frac{1}{|\mathcal{E}_2^U|}$ for all columns ($\forall e_j \in \mathcal{E}_2^U$). Assume that $|\mathcal{E}_1^U| < |\mathcal{E}_2^U|$, the decision threshold is $\frac{1}{2 \cdot \min(|\mathcal{E}_1^U|, |\mathcal{E}_2^U|)} = \frac{1}{2|\mathcal{E}_1^U|}$. Entity pairs $\{(e_i, e_j) \mid \mathbf{P}_{e_i, e_j}^* > \frac{1}{2|\mathcal{E}_1^U|}, e_i \in \mathcal{E}_1^U, e_j \in \mathcal{E}_2^U\}$ are selected as pseudo-labeled alignments.

For each pseudo-labeled alignment (e_i, e_j) with a probability value $\mathbf{P}_{e_i, e_j}^* > \frac{1}{2|\mathcal{E}_1^U|}$, we can prove that no conflicted entity pairs $\{(e_i, e_k) \mid e_k \in \mathcal{E}_2^U \setminus \{e_j\}\}$ associated with e_i are selected as pseudo-labeled alignments:

$$\begin{aligned} \mathbf{P}_{e_i, e_j}^* &> \frac{1}{2|\mathcal{E}_1^U|}, \\ \sum_{e_j \in \mathcal{E}_2^U} \mathbf{P}_{e_i, e_j}^* - \mathbf{P}_{e_i, e_j}^* &< \sum_{e_j \in \mathcal{E}_2^U} \mathbf{P}_{e_i, e_j}^* - \frac{1}{2|\mathcal{E}_1^U|}, \\ \sum_{e_k \in \mathcal{E}_2^U \setminus \{e_j\}} \mathbf{P}_{e_i, e_k}^* + \mathbf{P}_{e_i, e_j}^* - \mathbf{P}_{e_i, e_j}^* &< \frac{1}{|\mathcal{E}_1^U|} - \frac{1}{2|\mathcal{E}_1^U|}, \\ \sum_{e_k \in \mathcal{E}_2^U \setminus \{e_j\}} \mathbf{P}_{e_i, e_k}^* &< \frac{1}{2|\mathcal{E}_1^U|}. \end{aligned} \quad (13)$$

Since the coupling matrix $\mathbf{P}^* \in \mathbb{R}_+^{|\mathcal{E}_1^U| \times |\mathcal{E}_2^U|}$ has non-negative entries, the summation $\sum_{e_k \in \mathcal{E}_2^U \setminus \{e_j\}} \mathbf{P}_{e_i, e_k}^*$ from Eq. (13) must be no smaller than any component of it, i.e., $\mathbf{P}_{e_i, e_k}^* \leq \sum_{e_k \in \mathcal{E}_2^U \setminus \{e_j\}} \mathbf{P}_{e_i, e_k}^*, \forall e_k \in \mathcal{E}_2^U \setminus \{e_j\}$. Together with Eq. (13), we can further derive that any component in the summation is smaller than the decision threshold, i.e., $\mathbf{P}_{e_i, e_k}^* \leq \sum_{e_k \in \mathcal{E}_2^U \setminus \{e_j\}} \mathbf{P}_{e_i, e_k}^* < \frac{1}{2|\mathcal{E}_1^U|}, \forall e_k \in \mathcal{E}_2^U \setminus \{e_j\}$. In other words, all other probability values in the same row of \mathbf{P}_{e_i, e_j}^* are smaller than the decision threshold. Thus, no conflicted entity pairs $\{(e_i, e_k) \mid e_k \in \mathcal{E}_2^U \setminus \{e_j\}\}$ associated with e_i are selected as pseudo-labeled alignments.

Similarly, for each pseudo-labeled alignment (e_i, e_j) with a probability value $\mathbf{P}_{e_i, e_j}^* > \frac{1}{2|\mathcal{E}_1^U|}$, we can prove that no conflicted entity pairs $\{(e_l, e_j) \mid e_l \in \mathcal{E}_1^U \setminus \{e_i\}\}$ associated with entity e_j are selected as pseudo-labeled alignments. Similar to Eq. (13), we can also obtain $\sum_{e_l \in \mathcal{E}_1^U \setminus \{e_i\}} \mathbf{P}_{e_l, e_j}^* < \frac{1}{2|\mathcal{E}_2^U|}$ and $\mathbf{P}_{e_l, e_j}^* \leq \sum_{e_l \in \mathcal{E}_1^U \setminus \{e_i\}} \mathbf{P}_{e_l, e_j}^*, \forall e_l \in \mathcal{E}_1^U \setminus \{e_i\}$. Together with the assumption of $|\mathcal{E}_1^U| < |\mathcal{E}_2^U|$, we can further derive that $\mathbf{P}_{e_l, e_j}^* \leq \sum_{e_l \in \mathcal{E}_1^U \setminus \{e_i\}} \mathbf{P}_{e_l, e_j}^* < \frac{1}{2|\mathcal{E}_2^U|} < \frac{1}{2|\mathcal{E}_1^U|}$. Therefore, all other probability values in the same column of \mathbf{P}_{e_i, e_j}^* are smaller than the decision threshold, i.e., $\mathbf{P}_{e_l, e_j}^* < \frac{1}{2|\mathcal{E}_1^U|}, \forall e_l \in \mathcal{E}_1^U \setminus \{e_i\}$. Hence, no conflicted entity pairs $\{(e_l, e_j) \mid e_l \in \mathcal{E}_1^U \setminus \{e_i\}\}$ associated with entity e_j are selected as pseudo-labeled alignments.

In summary, we conclude that the selected pseudo-labeled alignments $\{(e_i, e_j) \mid \mathbf{P}_{e_i, e_j}^* > \frac{1}{2 \cdot \min(|\mathcal{E}_1^U|, |\mathcal{E}_2^U|)}, e_i \in \mathcal{E}_1^U, e_j \in \mathcal{E}_2^U\}$ are guaranteed to be one-to-one alignments when $|\mathcal{E}_1^U| < |\mathcal{E}_2^U|$, and the same conclusion also holds when $|\mathcal{E}_1^U| \geq |\mathcal{E}_2^U|$. \square

The OT-based pseudo-labeling algorithm is provided in Algorithm 1. In Step 1, the algorithm starts by calculating the transport cost matrix \mathbf{C} , with a time complexity of $O(|\mathcal{E}_1^U| \cdot |\mathcal{E}_2^U| \cdot d)$, where d is the embedding dimension. In Steps 2-9, the Sinkhorn algorithm takes the transport cost matrix \mathbf{C} as input to estimate the optimal transport plan \mathbf{P}^* via iterative row normalization and column normalization, the time complexity is $O(|\mathcal{E}_1^U| \cdot |\mathcal{E}_2^U| / \beta)$. In Step 10, entity pairs with values in \mathbf{P}^* larger than the decision threshold are selected as pseudo-labeled alignments. Finally, in Step 11, the algorithm returns a set of pseudo-labeled alignments $\hat{\mathcal{S}}_t$. The overall time complexity of Algorithm 1 is $O(|\mathcal{E}_1^U| \cdot |\mathcal{E}_2^U| \cdot d)$.

Algorithm 1: OT-based Pseudo-labeling with Sinkhorn Algorithm

Input: Unaligned entity sets $\mathcal{E}_1^U \subset \mathcal{E}_1$ and $\mathcal{E}_2^U \subset \mathcal{E}_2$, entity embeddings $\{\mathbf{h}_i \mid e_i \in \mathcal{E}_1^U \cup \mathcal{E}_2^U\}$ and regularization hyper-parameter β .

Output: Pseudo-labeled alignments $\hat{\mathcal{S}}_t$

- 1 Calculate transport cost \mathbf{C} according to Eq. (8);
 - 2 Initialize $\mathbf{P} = \mathbf{1}_{|\mathcal{E}_1^U|} \mathbf{1}_{|\mathcal{E}_2^U|}^\top$;
 - 3 $\mathbf{a} = \frac{1}{|\mathcal{E}_1^U|} \mathbf{1}_{|\mathcal{E}_1^U|}, \mathbf{Z} = e^{-\frac{1}{\beta} \mathbf{C}}$;
 - 4 **repeat**
 - 5 $\mathbf{Q} = \mathbf{Z} \odot \mathbf{P}$;
 - 6 $\mathbf{b} = \frac{1}{|\mathcal{E}_1^U| \mathbf{Q}^\top \mathbf{a}}, \mathbf{a} = \frac{1}{|\mathcal{E}_2^U| \mathbf{Q} \mathbf{b}}$;
 - 7 $\mathbf{P} = \mathbf{a} \mathbf{b}^\top \odot \mathbf{Q}$;
 - 8 **until** convergence or reaching a fixed number of iterations;
 - 9 Obtain the optimal transport plan $\mathbf{P}^* = \mathbf{P}$;
 - 10 Select conflict-free pseudo-labeled alignments
 - $\hat{\mathcal{S}}_t = \{(e_i, e_j) \mid \mathbf{P}_{e_i, e_j}^* > \frac{1}{2 \cdot \min(|\mathcal{E}_1^U|, |\mathcal{E}_2^U|)}, e_i \in \mathcal{E}_1^U, e_j \in \mathcal{E}_2^U\}$;
 - 11 **return** pseudo-labeled alignments $\hat{\mathcal{S}}_t$.
-

After obtaining the set of pseudo-labeled alignments $\widehat{\mathcal{S}}_t$, seed alignments are updated as $\mathcal{S} \leftarrow \mathcal{S}_0 \cup \widehat{\mathcal{S}}_t$ for training the EA model in the next iteration. To distinguish the contributions of pseudo-labeled alignments $\widehat{\mathcal{S}}_t$ from the prior seed alignments \mathcal{S}_0 provided beforehand during model training, we assign a soft weighting score to each alignment provided for training, defined as follows:

$$w(e_i, e_j) = \begin{cases} 1, & (e_i, e_j) \in \mathcal{S}_0, \\ 1/(1 + e^{\mathcal{C}_{e_i, e_j}}), & (e_i, e_j) \in \widehat{\mathcal{S}}_t. \end{cases} \quad (14)$$

For each pseudo-labeled alignment $(e_i, e_j) \in \widehat{\mathcal{S}}_t$, its weighting score $w(e_i, e_j)$ is within the range of $(0, 1)$ and inversely related to the transport cost \mathcal{C}_{e_i, e_j} . This ensures that the contribution of each pseudo-labeled alignment is appropriately moderated compared to the ground truth alignments during model training. Accordingly, the margin-based loss function for embedding learning, defined in Eq. (5), is updated as follows:

$$L = \sum_{(e_i, e_j) \in \mathcal{S}} \sum_{(e_i^-, e_j^-) \in \mathcal{S}_{(e_i, e_j)}^-} w(e_i, e_j) \cdot \max(0, d(e_i, e_j) - d(e_i^-, e_j^-) + \gamma). \quad (15)$$

3.2.2 Pseudo-Label Ensembling

Through OT-based pseudo-labeling, a set of conflict-free pseudo-labeled alignments are inferred at each iteration. However, they are still susceptible to one-to-one misalignments (Type II pseudo-labeling errors), especially when the learned entity embeddings are uninformative at early training stages. To address this issue, we propose a self-ensembling approach that refines pseudo-labeled alignments by combining predictions over multiple pseudo-labeling iterations. The objective is to seek consensus predictions over multiple iterations to reduce the prediction variability, thereby improving the quality of pseudo-labeled alignments.

Formally, given m sets of pseudo-labeled alignments $\{\widehat{\mathcal{S}}_t | t = 1, \dots, m\}$ inferred from every m consecutive iterations, we generate pseudo-labeled alignments that are commonly selected in all of $\{\widehat{\mathcal{S}}_t | t = 1, \dots, m\}$:

$$\widehat{\mathcal{S}} = \bigcap_{t=1}^m \widehat{\mathcal{S}}_t = \{(e_i, e_j) | \sum_{t=1}^m \mathbb{1}((e_i, e_j) \in \widehat{\mathcal{S}}_t) = m, e_i \in \mathcal{E}_1^U, e_j \in \mathcal{E}_2^U\}, \quad (16)$$

where $\mathbb{1}(\cdot)$ is a binary indicator function. To decorrelate the dependency among m consecutive iterations, model parameters are randomly reinitialized during each of these iterations (Cascante-Bonilla et al, 2021).

By focusing on consensus alignments across iterations, our self-ensembling approach is expected to have higher pseudo-labeling precision than using the predictions from the most recent iteration alone. This approach is related to self-ensembling techniques like temporal ensembling (Laine and Aila, 2017), which uses exponential

moving average smoothing to aggregate model predictions across iterations and adds regularization to the loss function to improve prediction consistency on unlabeled data. Our approach shares the same objective but provides a simple yet effective solution, which also supports UPL-EA’s utility to integrate with other EA models (as empirically demonstrated in Section 4.3.2 and 4.3.3).

Finally, the refined pseudo-labeled alignments $\widehat{\mathcal{S}}$ are used to augment prior seed alignments \mathcal{S}_0 as follows:

$$\mathcal{S}_0 \leftarrow \mathcal{S}_0 \cup \widehat{\mathcal{S}}. \quad (17)$$

The augmented set \mathcal{S}_0 includes a considerable number of reliable pseudo-labeled alignments, which in turn strengthens subsequent model training.

3.3 Overall Workflow

The training process of UPL-EA is summarized in Algorithm 2. In Steps 2-5, the EA model and OT-Based pseudo-labeling alternately reinforce each other to learn informative entity embeddings. In Steps 6-7, the pseudo-label ensembling is performed every m iterations to augment prior seed alignments with reliably selected pseudo-labeled alignments for subsequent training. Finally, the learned entity embeddings are returned as the output. For alignment inference, the learned entity embeddings are used to infer new aligned entity pairs via Algorithm 1.

Algorithm 2: UPL-EA Training Process

Input: Two KGs $\mathcal{G}_1 = \{\mathcal{E}_1, \mathcal{R}_1, \mathcal{T}_1\}$, $\mathcal{G}_2 = \{\mathcal{E}_2, \mathcal{R}_2, \mathcal{T}_2\}$, prior seed alignments \mathcal{S}_0 .
Output: Learned entity embeddings.

- 1 **repeat**
- 2 **for** t in $1 \dots m$ **do**
- 3 Infer pseudo-labeled alignments $\widehat{\mathcal{S}}_t$ via Algorithm 1;
- 4 Augment seed alignments: $\mathcal{S} \leftarrow \mathcal{S}_0 \cup \widehat{\mathcal{S}}_t$;
- 5 Learn entity embeddings by minimizing the loss function in Eq. (15);
- 6 Ensemble pseudo-labeled alignments $\widehat{\mathcal{S}} = \bigcap_{t=1}^m \widehat{\mathcal{S}}_t$;
- 7 Augment prior seed alignments: $\mathcal{S}_0 \leftarrow \mathcal{S}_0 \cup \widehat{\mathcal{S}}$;
- 8 **until** convergence or reaching a fixed number of iterations;
- 9 **return** learned entity embeddings.

In Algorithm 2, the time complexity of OT-based pseudo-labeling in Step 3 is $O(|\mathcal{E}_1^U| \cdot |\mathcal{E}_2^U| \cdot d)$, where d is the entity embedding dimension, and the time complexity of learning entity embeddings in Step 5 is $O((|\mathcal{E}_1 \cup \mathcal{E}_2|) \cdot d^2)$. Thus, the time complexity of Algorithm 2 is $O(I \cdot (|\mathcal{E}_1^U| \cdot |\mathcal{E}_2^U| \cdot d + (|\mathcal{E}_1 \cup \mathcal{E}_2|) \cdot d^2))$, where I is the maximum number of iterations.

4 Experiments

In this section, we validate the efficacy of our proposed UPL-EA framework through extensive experiments, ablation studies and in-depth analyses on benchmark datasets.

4.1 Experimental Settings

4.1.1 Datasets

To evaluate the effectiveness of our UPL-EA framework, we carry out experiments on both cross-lingual datasets and cross-source monolingual datasets. The statistics of all datasets are summarized in Table 1.

Table 1: Statistics of benchmark datasets

Datasets		Entities	Relations	Rel.triplets
DBP15K _{ZH_EN}	Chinese	66,469	2,830	153,929
	English	98,125	2,317	237,674
DBP15K _{JA_EN}	Japanese	65,744	2,043	164,373
	English	95,680	2,096	233,319
DBP15K _{FR_EN}	French	66,858	1,379	192,191
	English	105,889	2,209	278,590
SRPRS _{EN_FR}	English	15,000	221	36,508
	French	15,000	177	33,532
SRPRS _{EN_DE}	English	15,000	222	38,363
	German	15,000	120	37,377
DBP-YG-15K (OpenEA)	English	15,000	165	30,291
	English	15,000	28	26,638
DBP-YG-15K (RealEA)	English	19,865	290	60,329
	English	21,050	32	82,109

Cross-lingual Datasets. DBP15K (Sun et al, 2017) is a widely used benchmark dataset for cross-lingual entity alignment (Ding et al, 2022; Liu et al, 2022; Wu et al, 2019a; Zhu et al, 2021). It includes three cross-lingual KG pairs extracted from DBpedia, each containing two KGs built upon English and another language (Chinese, Japanese, or French), with 15,000 aligned entity pairs per dataset. SRPRS (Guo et al, 2019) is a more recent benchmark dataset characterized by sparser connections (Guo et al, 2019) that are extracted from DBpedia. SRPRS comprises two cross-lingual KG pairs, each with two KGs in English and French/German, and also includes 15,000 aligned entity pairs.

Cross-Source Monolingual Datasets. DBP-YG-15K is a cross-source monolingual dataset extracted from DBpedia (Auer et al, 2007) and YAGO 3 (Suchanek et al, 2007). DBP-YG-15K has two KG pairs, sampled by OpenEA (Sun et al, 2020b) and RealEA (Leone et al, 2022), respectively. The OpenEA KG pair is constructed without duplicated entities in each KG, which aligns with our approach. However, the RealEA

KG pair does not use this setting and allow duplicated entities in one KG. Both KG pairs of DBP-YG-15K are built upon English and each has 15,000 aligned entity pairs.

4.1.2 Experimental Setup

For fair comparisons, we follow the conventional 30%-70% split ratio to randomly partition training and test data on all datasets. We use semantic meanings of entity names to construct entity features. On DBP15K with relatively larger linguistic barriers, we first use Google Translate to translate non-English entity names into English, then look up 768-dimensional word embeddings pre-trained by BERT (Devlin et al, 2019) with English entity names to form entity features. On SRPRS and DPB-YG-15K, we directly look up word embeddings without translation. As each entity name comprises one or multiple words, we further use TF-IDF to measure the contribution of each word towards entity name representation. Finally, we aggregate TF-IDF-weighted word embeddings for each entity to form its entity feature vector.

The settings of UPL-EA are specified as follows: $K = 125$, $\beta = 0.5$, $\gamma = 1$, $\lambda = 10$, and $m = 3$. The embedding dimension d is set to 300. For BERT pre-trained word embeddings, we use a PCA-based technique (Raunak et al, 2019) to reduce feature dimension from 768 to 300 with minimal information loss. The number of pseudo-labeling iterations is set to 10, where each iteration contains 10 training epochs for the EA model. We implement our model in PyTorch, using the Adam optimizer with a learning rate of 0.001 on DBP15K and DBP-YG-15K, and 0.00025 on SRPRS. The batch size is set to 256. All experiments are run on a computer with an Intel(R) Core(TM) i9-13900KF CPU @ 3.00GHz and an NVIDIA Geforce RTX 4090 (24GB memory) GPU.

4.2 Comparison with State-of-the-Art Baselines

To thoroughly validate the effectiveness and applicability of UPL-EA, we compare it with a series of state-of-the-art baselines on both cross-lingual and cross-source monolingual datasets.

4.2.1 Results on Cross-lingual Datasets

On cross-lingual datasets, language differences could impact the difficulty of aligning entities across different linguistic KGs. Following the survey paper by Zhao et al (2020), we use the term of linguistic barriers to indicate inherent differences in language uses related to syntactic structures, semantic divergences and cultural nuances encoded in languages (Motschenbacher, 2022). For example, DBP15K_{ZH_EN} (Chinese-English) and DBP15K_{JA_EN} (Japanese-English) are considered as distantly-related languages with larger language barriers. whereas DBP15K_{FR_EN} (French-English), SRPRS_{EN_FR} (English-French) and SRPRS_{EN_DE} are considered as closely-related languages with smaller language barriers.

Baselines and Metrics. We compare UPL-EA with 12 state-of-the-art EA models on cross-lingual datasets: DBP15K and SRPRS, which broadly fall into two categories:

Table 2: Performance comparison on DBP15K. The asterisk (*) indicates that semantic meanings of entity names are used to construct entity features. The best and second best results per column are highlighted in **bold** and underlined, respectively.

Models	DBP15K _{ZH_EN}			DBP15K _{JA_EN}			DBP15K _{FR_EN}		
	Hit@1	Hit@10	MRR	Hit@1	Hit@10	MRR	Hit@1	Hit@10	MRR
MTransE	20.9	51.2	0.31	25.0	57.2	0.36	24.7	57.7	0.36
JAPE-Stru	37.2	68.9	0.48	32.9	63.8	0.43	29.3	61.7	0.40
GCN-Stru	39.8	72.0	0.51	40.0	72.9	0.51	38.9	74.9	0.51
JAPE*	41.4	74.1	0.53	36.5	69.5	0.48	31.8	66.8	0.44
GCN-Align*	43.4	76.2	0.55	42.7	76.2	0.54	41.1	77.2	0.53
HMAN*	56.1	85.9	0.67	55.7	86.0	0.67	55.0	87.6	0.66
RDGCN*	69.7	84.2	0.75	76.3	89.7	0.81	87.3	95.0	0.90
HGCN*	70.8	84.0	0.76	75.8	88.9	0.81	88.8	95.9	0.91
CEA*	78.7	-	-	86.3	-	-	97.2	-	-
IPTransE	33.2	64.5	0.43	29.0	59.5	0.39	24.5	56.8	0.35
BootEA	61.4	84.1	0.69	57.3	82.9	0.66	58.5	84.5	0.68
MRAEA	75.7	93.0	0.83	75.8	93.4	0.83	78.0	94.8	0.85
RNM*	84.0	91.9	0.87	87.2	94.4	0.90	93.8	98.1	0.95
CPL-OT*	<u>92.7</u>	<u>96.4</u>	<u>0.94</u>	<u>95.6</u>	<u>98.3</u>	<u>0.97</u>	<u>99.0</u>	<u>99.4</u>	<u>0.99</u>
UPL-EA*	94.9	97.4	0.96	97.0	98.8	0.98	99.5	99.7	1.00

- Supervised models, including MTransE (Chen et al, 2017), JAPE (Sun et al, 2017), JAPE in its structure-only variant denoted as JAPE-Stru, GCN-Align (Wang et al, 2018), GCN-Align in its structure-only variant denoted as GCN-Stru, RDGCN (Wu et al, 2019a), HGCN (Wu et al, 2019b), HMAN (Yang et al, 2019), and CEA (Zeng et al, 2020);
- Pseudo-labeling-based models, including IPTransE (Zhu et al, 2017), BootEA (Sun et al, 2018), MRAEA (Mao et al, 2020), RNM (Zhu et al, 2021), and CPL-OT (Ding et al, 2022).

The results of MRAEA and CPL-OT on both datasets, and RNM on DBP15K are obtained from their original papers. Results of other baselines are obtained from (Zhao et al, 2020). For UPL-EA, we report the average results over five runs.

Following the evaluation protocols of mainstream state-of-the-art EA models, we utilize ranking-based metrics: Hit@k ($k = 1, 10$) and Mean Reciprocal Rank (MRR), on cross-lingual datasets. Given a set of test alignments $\mathcal{S}_{\text{test}}$, Hit@k measures the percentage of correctly aligned entity pairs where the true corresponding counterpart of a source entity appears within the top-k positions in the list of candidate counterparts. MRR measures the average of the reciprocal ranks for the correctly aligned entities. Higher Hit@k and MRR scores indicate better EA performance.

The Results. Table 2 and Table 3 report performance comparisons on DBP15K and SRPRS, respectively. This set of results are reported with 30% prior seed alignments used for training. The asterisk (*) indicates that semantic meanings of entity names are used to construct entity features.

Our results show that UPL-EA significantly outperforms most existing EA models on five cross-lingual KG pairs. In particular, on DBP15K_{ZH_EN}, UPL-EA outperforms the second and third performers, CPL-OT and RNM, by over 2% and 10%,

Table 3: Performance comparison on SRPRS. The asterisk (*) indicates that semantic meanings of entity names are used to construct entity features. The best and second best results per column are highlighted in **bold** and underlined, respectively.

Models	SRPRS _{EN_FR}			SRPRS _{EN_DE}		
	Hit@1	Hit@10	MRR	Hit@1	Hit@10	MRR
MtransE	21.3	44.7	0.29	10.7	24.8	0.16
JAPE-Stru	24.1	53.3	0.34	30.2	57.8	0.40
GCN-Stru	24.3	52.2	0.34	38.5	60.0	0.46
JAPE*	24.1	54.4	0.34	26.8	54.7	0.36
GCN-Align*	29.6	59.2	0.40	42.8	66.2	0.51
HMAN*	40.0	70.5	0.50	52.8	77.8	0.62
RDGCN*	67.2	76.7	0.71	77.9	88.6	0.82
HGCN*	67.0	77.0	0.71	76.3	86.3	0.80
CEA*	96.2	-	-	97.1	-	-
IPTransE	12.4	30.1	0.18	13.5	31.6	0.20
BootEA	36.5	64.9	0.46	50.3	73.2	0.58
MRAEA	46.0	76.8	0.56	59.4	81.5	0.66
RNM*	92.5	96.2	0.94	94.4	96.7	0.95
CPL-OT*	<u>97.4</u>	<u>98.8</u>	<u>0.98</u>	<u>97.4</u>	<u>98.9</u>	<u>0.98</u>
UPL-EA*	98.2	99.3	0.99	98.4	99.5	0.99

respectively, in terms of Hit@1. This affirms the necessity of systematically combating confirmation bias for pseudo-labeling-based entity alignment. It is worth noting that disparities in overall performance can be observed among the five cross-lingual KG pairs, where the lowest accuracy is achieved on DBP15K_{ZH_EN} due to its large linguistic barriers. Nevertheless, for the most challenging EA task on DBP15K_{ZH_EN}, UPL-EA yields strong performance gains over other baselines.

4.2.2 Results on Cross-Source Monolingual Datasets

Baselines and Metrics. On monolingual dataset DBP-YG-15K, we compare UPL-EA with five EA models, including BootEA (Sun et al, 2018), RDGCN (Wu et al, 2019a), BERT-INT (Tang et al, 2021), TransEdge (Sun et al, 2019), and PARIS+ (Leone et al, 2022). The results of these baselines are obtained from (Leone et al, 2022). BootEA, TransEdge, and UPL-EA use relational triplets only, the same as our setting. PARIS+, RDGCN, and BERT-INT use both relational and attribute triplets. For UPL-EA, we report the average results over five runs.

For more comprehensive evaluation, we adopt classification-based metrics suggested by Leone et al (2022) on DBP-YG-15K, which are precision, recall, and F_1 score. Given a set of alignments inferred by an EA model $\mathcal{S}_{\text{pred}}$ and a set of test alignments $\mathcal{S}_{\text{test}}$, the three classification-based metrics are calculated as follows:

$$\text{Precision} = \frac{|\mathcal{S}_{\text{pred}} \cap \mathcal{S}_{\text{test}}|}{|\mathcal{S}_{\text{pred}}|}, \text{Recall} = \frac{|\mathcal{S}_{\text{pred}} \cap \mathcal{S}_{\text{test}}|}{|\mathcal{S}_{\text{test}}|}, F_1 = 2 \times \frac{\text{Precision} \times \text{Recall}}{\text{Precision} + \text{Recall}}.$$

The Results. Table 4 reports performance comparisons on DBP-YG-15K (OpenEA) and DBP-YG-15K (RealEA) with 30% prior seed alignments used for training. The asterisk “*” indicates that semantic meanings of entity names are used in EA modeling. Our results show that UPL-EA outperforms all five baselines across two KG pairs of DBP-YG-15K. On the OpenEA KG pair, UPL-EA achieves nearly perfect performance with all three metrics to be approximately 1, outperforming the second best baseline by more than 2% on F_1 score. On the RealEA KG pair of DBP-YG-15K, even with duplicated entities in each KG (Leone et al, 2022), UPL-EA performs competitively with an over 3% improvement on F_1 score compared to the second best baseline.

Table 4: Performance comparison on DBP-YG-15K. The asterisk “*” indicates that semantic meanings of entity names are used in EA modeling. The best and second best results per column are highlighted in **bold** and underlined, respectively.

	DBP-YG-15K (OpenEA)			DBP-YG-15K (RealEA)		
	Precision	Recall	F_1 -score	Precision	Recall	F_1 -score
TransEdge	0.367	0.212	0.268	0.335	0.203	0.253
BootEA	0.926	0.675	0.781	0.459	0.313	0.372
RDGCN*	0.984	0.855	0.915	0.822	0.709	0.761
BERT-INT*	0.875	<u>0.969</u>	0.920	0.817	0.827	0.822
PARIS+*	<u>0.998</u>	0.961	<u>0.979</u>	<u>0.906</u>	0.931	<u>0.918</u>
UPL-EA*	1.000	1.000	1.000	0.973	0.931	0.952

Our reported results on both cross-lingual and cross-source monolingual datasets thus far demonstrate the viability of UPL-EA across various datasets. We will then focus on cross-lingual datasets DBP15K and SRPRS for subsequent experiments and analyses, as cross-lingual contexts present complexities like linguistic barriers, which are crucial for assessing the efficacy of our proposed framework.

4.3 Ablation Studies and Analyses

4.3.1 Effectiveness of Different Components

To assess the importance of various components of the proposed UPL-EA framework, we conduct a series of ablation studies on five cross-lingual KG pairs from DBP15K and SRPRS. To provide deeper insights, we undertake ablation studies under two settings: the conventional setting using 30% prior seed alignments and the setting with no prior seed alignments provided. The full UPL-EA model is compared with its ablated variants, with the best performance highlighted by **bold**. From Table 5 and Table 6, we can see that the full UPL-EA model performs the best in all cases.

- **w.o. Global-lev. Rel. Aggr.:** We compare the full UPL-EA model against the variant without using global-level relation aggregation for entity embedding learning. This ablation leads to degraded performance on both settings primarily due to the increase in conflicted misalignments caused by feature over-smoothing.
- **w.o. Dist. Rectification:** The effectiveness of embedding distance rectification is examined by using the original embedding distance defined in Eq. (6) as the

Table 5: Ablation study on DBP15K

Models	DBP15K _{ZH_EN}			DBP15K _{JA_EN}			DBP15K _{FR_EN}		
	Hit@1	Hit@10	MRR	Hit@1	Hit@10	MRR	Hit@1	Hit@10	MRR
30% prior seed alignments									
Full Model	94.9	97.4	0.96	97.0	98.8	0.98	99.5	99.7	1.00
w.o. Global-lev. Rel. Aggr.	92.6	96.4	0.94	96.4	98.5	0.97	99.3	99.7	1.00
w.o. Dist. Rectification	82.6	89.6	0.85	89.8	94.5	0.91	96.8	98.0	0.97
w.o. OT. Pseudo-Labeling	80.1	90.4	0.84	87.6	94.8	0.90	94.4	97.4	0.96
w.o. Pseudo-Label Ensemb.	84.9	90.6	0.87	91.1	95.5	0.93	98.1	99.0	0.98
w.o. OT. & Ensemb.	74.8	87.3	0.80	83.4	93.6	0.87	93.1	97.5	0.95
No prior seed alignments									
Full Model	93.1	96.2	0.94	95.7	98.3	0.97	99.2	99.5	0.99
w.o. Global-lev. Rel. Aggr.	91.4	95.3	0.93	95.3	98.1	0.96	99.1	99.7	0.99
w.o. Dist. Rectification	72.5	79.9	0.75	82.5	89.2	0.85	95.4	97.2	0.96
w.o. OT. Pseudo-Labeling	66.9	75.5	0.70	76.9	85.2	0.80	91.9	95.2	0.93
w.o. Pseudo-Label Ensemb.	83.0	88.7	0.85	90.1	94.6	0.92	97.8	98.8	0.98
w.o. OT. & Ensemb.	67.1	76.8	0.71	77.1	86.2	0.81	91.4	95.9	0.93

Table 6: Ablation study on SRPRS

Models	SRPRS _{EN_FR}			SRPRS _{EN_DE}		
	Hit@1	Hit@10	MRR	Hit@1	Hit@10	MRR
30% prior seed alignments						
Full Model	98.2	99.3	0.99	98.4	99.5	0.99
w.o. Global-lev. Rel. Aggr.	97.5	98.9	0.98	97.8	99.2	0.98
w.o. Dist. Rectification	95.1	96.7	0.96	97.0	98.2	0.97
w.o. OT. Pseudo-Labeling	93.9	96.6	0.95	94.2	97.5	0.95
w.o. Pseudo-Label Ensemb.	94.6	97.4	0.96	94.8	98.1	0.96
w.o. OT. & Ensemb.	92.7	96.5	0.94	93.6	97.4	0.95
No prior seed alignments						
Full Model	97.9	99.2	0.98	97.7	99.2	0.98
w.o. Global-lev. Rel. Aggr.	97.1	98.6	0.98	97.4	98.7	0.98
w.o. Dist. Rectification	93.0	94.7	0.94	94.9	97.0	0.96
w.o. OT. Pseudo-Labeling	89.8	93.0	0.91	91.4	95.2	0.93
w.o. Pseudo-Label Ensemb.	94.2	97.0	0.95	94.8	97.7	0.96
w.o. OT. & Ensemb.	89.7	93.1	0.91	91.1	94.9	0.93

transport cost used for OT modeling. The ablation of distance rectification leads to a significant performance drop at both settings. This highlights the complementary role of distance rectification in the training of the EA model, particularly during the early stages, for learning more informative entity embeddings and providing a reliable cost measure for OT modeling.

- **w.o. OT. Pseudo-Labeling:** To study the efficacy of OT-based Pseudo-Labeling, we ablate it from the full UPL-EA model. As OT modeling can effectively eliminate a considerable number of Type I pseudo-labeling errors to

ensure one-to-one correspondences at each iteration, this ablation results in a profound performance drop across all datasets on both settings.

- **w.o. Pseudo-Label Ensemb.:** The ablation of pseudo-label ensembling from UPL-EA also significantly degrades alignment performance, with substantial performance declines observed in both settings, especially on DBP15K_{ZH_EN} and DBP15K_{JA_EN} with large linguistic barriers. In contrast, performance drops are less pronounced on DBP15K_{FR_EN}, SRPRS_{EN_FR}, and SRPRS_{EN_DE} with relatively small linguistic barriers. This is attributed to the fact that larger linguistic barriers tend to incur more one-to-one misalignments (Type II pseudo-labeling errors). Our findings confirm that pseudo-label ensembling is crucial for UPL-EA to achieve its full potential, especially when model predictions are less accurate during early training stages.
- **w.o. OT. & Ensemb.:** We also analyze the overall effect of ablating both OT modeling and pseudo-label ensembling from the full model. This ablation, conceptually identical to the naive pseudo-labeling strategy (Sun et al, 2019), has a substantial adverse impact, leading to a dramatic performance drop in all cases. Our results highlight the effectiveness of our proposed UPL-EA framework in systematically combating confirmation bias for pseudo-labeling-based entity alignment.

Note that under the setting with no prior seed alignments, the variant without OT-based pseudo-labeling (w.o. OT. Pseudo-Labeling) has similar performance as compared to the variant completely ignoring confirmation bias (w.o. OT. & Ensemb.). In particular, on DBP15K_{ZH_EN} and DBP15K_{JA_EN}, the former variant even performs slightly worse. This is because under the challenging case where there are no prior seed alignments, ablating OT-based pseudo-labeling might incur considerably more conflicted misalignments (Type I pseudo-labeling errors). As a result, it becomes ineffective to refine erroneous pseudo-labeled alignments via ensembling.

4.3.2 Effectiveness as a General Pseudo-labeling Framework

To further demonstrate UPL-EA’s viability as a general pseudo-labeling framework for entity alignment, we substitute the EA model in UPL-EA (described in Section 3.1) with alternative EA models, and examine if applying our UPL strategy could bring any performance improvements. We consider two alternative EA models: (1) GCN-Align (Wang et al, 2018), which adopts a two-layer GCN as an encoder to learn entity embeddings, and (2) GAT-Align, where the GCN encoder in GCN-Align is replaced with a two-layer GAT for embedding learning. Both EA models use the same loss function provided in Eq. (5). This analysis is conducted on DBP15K with 30% prior seed alignments as a case study. The entity alignment performance using the two baselines and their UPL-EA augmented counterparts is reported in Table 7.

Our results in Table 7 indicate that applying UPL-EA to both GCN-Align and GAT-Align improves entity alignment performance by a considerable margin, with an average 20% improvement in Hit@1. Our results affirm the strong modular utility of UPL-EA as a general pseudo-labeling framework in boosting various EA models to achieve better alignment performance.

Table 7: Performance of UPL-EA instantiated with other EA models

	DBP15K _{ZH_EN}			DBP15K _{JA_EN}			DBP15K _{FR_EN}		
	Hit@1	Hit@10	MRR	Hit@1	Hit@10	MRR	Hit@1	Hit@10	MRR
GCN-Align	43.4	76.2	0.55	42.7	76.2	0.54	41.1	77.2	0.53
GCN _{UPL-EA}	79.8	91.5	0.84	82.5	94.2	0.87	87.0	96.8	0.91
GAT-Align	71.3	84.3	0.76	81.2	91.9	0.85	92.9	97.9	0.95
GAT _{UPL-EA}	92.2	96.8	0.94	93.6	98.1	0.95	98.3	99.6	0.99
UPL-EA	94.9	97.4	0.96	97.0	98.8	0.98	99.5	99.7	1.00

4.3.3 Comparisons with Other Pseudo-label Ensembling Methods

To investigate the effectiveness of UPL-EA’s pseudo-label ensembling, we carry out a case study on DBP15K using 30% prior seed alignments. Specifically, we compare the performance of UPL-EA with three pseudo-label ensembling methods: (1) consensus ensembling (our method), (2) majority vote, and (3) temporal ensembling (Laine and Aila, 2017). The entity alignment performance of UPL-EA using the three ensembling methods is reported in Table 8. Our results show that UPL-EA using our proposed consensus ensembling (UPL-EA_{C.E.}) consistently outperforms the variant using majority vote (UPL-EA_{M.V.}) and the variant using temporal ensembling (UPL-EA_{T.E.}).

Table 8: Performance of UPL-EA using different pseudo-Label ensembling methods.

	DBP15K _{ZH_EN}			DBP15K _{JA_EN}			DBP15K _{FR_EN}		
	Hit@1	Hit@10	MRR	Hit@1	Hit@10	MRR	Hit@1	Hit@10	MRR
UPL-EA _{C.E.}	94.9	97.4	0.96	97.0	98.8	0.98	99.5	99.7	1.00
UPL-EA _{M.V.}	93.7	96.4	0.95	96.6	98.5	0.97	99.3	99.6	0.99
UPL-EA _{T.E.}	92.8	95.3	0.94	96.0	97.6	0.97	98.7	99.0	0.99

To provide deeper insights into the performance of different pseudo-label ensembling methods, we explicitly evaluate the precision of pseudo-labeling using different ensembling methods on the test data, where the ground truth alignments are provided. Fig. 3 compares the precision of pseudo-labeling using three ensembling methods and without ensembling throughout pseudo-labeling iterations.

Notably, pseudo-labeling with ensembling methods consistently achieves higher precision compared to pseudo-labeling without ensembling throughout the training process. The performance gap is particularly significant on DBP15K_{ZH_EN} and DBP15K_{JA_EN}, where larger linguistic barriers exist. Without ensembling, the precision of pseudo-labeling initially increases but quickly plateaus at a sub-optimal level due to confirmation bias arising from the accumulation of one-to-one misalignments (Type II pseudo-labeling errors). In contrast, pseudo-label ensembling maintains a higher precision throughout the training process.

Among ensembling methods, the precision of pseudo-labeling with temporal ensembling initially increases by aggregating the first two iterations but gradually decreases as more iterations are used for ensembling. Majority vote consistently achieves higher

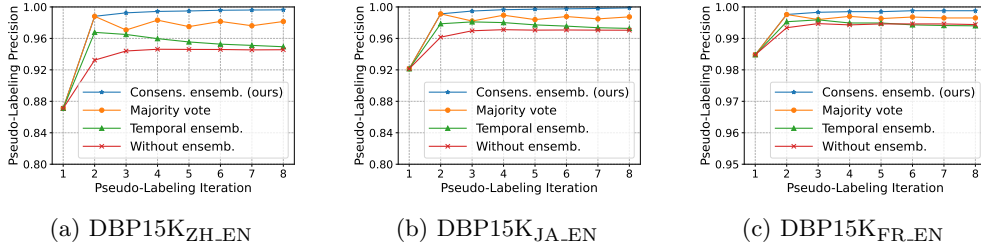


Fig. 3: Comparison with other pseudo-labeling ensembling methods.

precision than temporal ensembling, although its precision is unstable throughout the training process. Overall, consensus ensembling (ours) achieves nearly 100% precision after using only three iterations for ensembling across all KG pairs. Our findings suggest that UPL-EA’s pseudo-label ensembling provides a simple but effective way to improve the quality of pseudo-labeled alignments, achieving competitive performance compared to other ensembling methods.

4.4 Comparison w.r.t. Different Rates of Prior Seed Alignments

Next, we further examine how the performance of UPL-EA changes with respect to different rates of prior seed alignments, decreasing from 40% to 10%. We compare UPL-EA with four representative state-of-the-art baselines (BootEA, RDGCN, RNM, and CPL-OT), and report the results on DBP15K and SRPRS in Table 9 and Table 10. The last column “ $\Delta \downarrow$ ” in each table indicates the average performance loss when decreasing the rate from 40% to 10% for each model.

Table 9: Performance comparison (Hit@1) on DBP15K with respect to different rates of prior seed alignments. “ $\Delta \downarrow$ ” in the last column indicates the average performance loss when decreasing the rate from 40% to 10% on three datasets.

Models	DBP15K _{ZH_EN}				DBP15K _{JA_EN}				DBP15K _{FR_EN}				$\Delta \downarrow$
	40%	30%	20%	10%	40%	30%	20%	10%	40%	30%	20%	10%	
BootEA	67.9	62.9	57.3	45.7	66.0	62.2	53.5	42.9	68.6	65.3	59.8	47.3	-22.2
RDGCN	72.6	70.8	68.9	66.6	79.0	76.7	74.5	72.4	89.7	88.6	87.6	86.3	-5.3
RNM	85.4	84.0	81.7	79.3	88.8	87.2	85.9	83.4	94.5	93.8	93.0	92.3	-4.6
CPL-OT	93.0	92.7	92.2	91.8	96.1	95.6	95.1	94.7	99.2	99.1	98.9	98.7	-1.0
UPL-EA	95.2	94.9	94.1	93.6	97.4	97.0	96.8	96.4	99.5	99.5	99.4	99.2	-1.0

As expected, UPL-EA consistently outperforms four competitors on all cross-lingual KG pairs at all prior seed alignment rates. This is due to UPL-EA’s ability to augment the training set with reliable pseudo-labeled alignments by effectively alleviating confirmation bias. As the rate of prior seed alignments decreases from 40% to 10%, the performance of BootEA significantly degrades by over 20% on average due to its limited ability to prevent the accumulation of pseudo-labeling errors. RNM

Table 10: Performance comparison (Hit@1) on SRPRS with respect to different rates of prior seed alignments. “ $\Delta \downarrow$ ” in the last column indicates the average performance loss when decreasing the rate from 40% to 10% on two datasets.

Models	SRPRS _{EN_FR}				SRPRS _{EN_DE}				$\Delta \downarrow$
	40%	30%	20%	10%	40%	30%	20%	10%	
BootEA	39.9	36.5	31.1	18.3	53.6	50.3	43.3	32.8	-20.7
RDGCN	68.7	67.2	65.8	64.0	79.0	77.9	76.8	75.7	-3.2
RNM	93.6	92.5	90.4	89.3	95.0	94.4	93.8	92.9	-2.1
CPL-OT	97.6	97.4	97.3	97.1	97.6	97.4	97.2	97.0	-0.5
UPL-EA	98.3	98.2	98.0	97.8	98.4	98.4	97.7	97.4	-1.0

outperforms RDGCN owing to its posterior embedding distance editing during pseudo-labeling, however its lack of iterative model re-training hinders its overall performance. CPL-OT demonstrates more stable performance with varying rates of prior seed alignments because it selects pseudo-labeled alignments via the conflict-aware OT modeling and then uses them to train the EA model in turn; nevertheless, its neglect of one-to-one misalignments (Type II pseudo-labeling errors) limits the potential of CPL-OT. UPL-EA remains consistently competitive and stable across all datasets, with an average performance loss of 1% at most when the rate of prior seed alignments decreases from 40% to 10%, even on the most challenging DBP15K_{ZH_EN} dataset.

4.5 Impact of Pre-trained Word Embeddings

To analyze the impact of using different pre-trained word embeddings, we report the results of UPL-EA that form entity features with Glove embedding (Pennington et al, 2014), which is widely used in the existing EA models. We conduct this analysis on the setting with 30% prior seed alignments. The results on DBP15K are reported in Table 11 as a case study. We can observe that UPL-EA with Glove embedding still achieves competitive results, significantly outperforming all other baselines. This confirms that the efficacy of UPL-EA is not highly dependent on embedding initialization methods used. When switching from Glove embedding to BERT pre-trained embeddings, performance gains can be observed, especially on DBP15K_{JA_EN}. This indicates the usefulness of pre-trained word embeddings of high quality for entity alignment.

Table 11: Impact of pre-trained word embeddings

Models	DBP15K _{ZH_EN}			DBP15K _{JA_EN}			DBP15K _{FR_EN}		
	Hit@1	Hit@10	MRR	Hit@1	Hit@10	MRR	Hit@1	Hit@10	MRR
Glove	94.0	97.6	0.95	95.9	98.9	0.97	99.1	99.8	0.99
BERT	94.9	97.4	0.96	97.0	98.8	0.98	99.5	99.7	1.00

4.6 Hyper-parameter Sensitivity Analysis

We further study the sensitivity of UPL-EA with regards to four hyper-parameters: embedding dimension d , number of iterations m for pseudo-label ensembling, regularization hyper-parameter β in Eq. (11), and margin hyper-parameter γ in the alignment loss function Eq. (15). This set of sensitivity analysis is conducted on DBP15K_{ZH,EN} with 30% prior seed alignments as a case study. The respective results in terms of Hit@1 and Hit@10 are reported in Fig. 4.

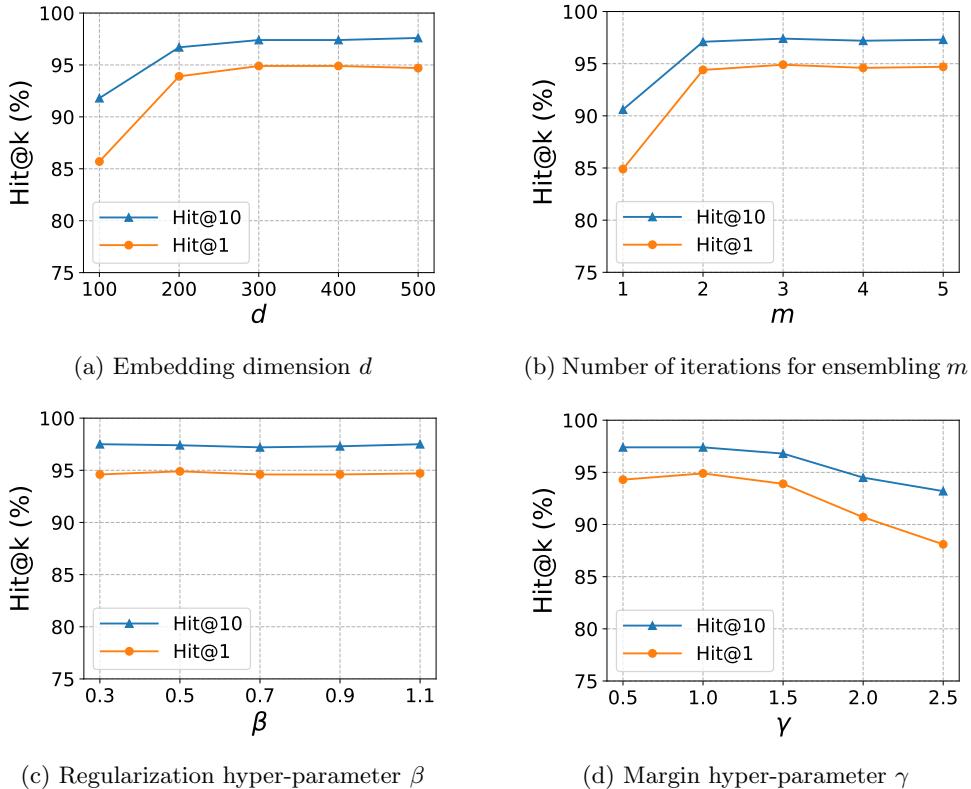


Fig. 4: Hyper-parameter sensitivity analysis on DBP15K_{ZH,EN}

As shown in Fig. 4a, the performance of UPL-EA improves considerably as the embedding dimension d increases from 100 to 300 and then retains at a relatively stable level. For the number of iterations m used for pseudo-label ensembling, the use of ensembling over multiple iterations ($m > 1$) significantly improves the alignment performance over a single iteration ($m = 1$). This demonstrates the effectiveness of our self-ensembling mechanism, which requires only a few iterations (e.g., $m = 3$) to achieve competitive performance (see Fig. 4b). In addition, Fig. 4c shows that the performance of UPL-EA is insensitive to different values of β used in OT-based

pseudo-labeling. As for the margin parameter γ , the performance of UPL-EA begins to drop gradually when γ exceeds 1, as shown in Fig. 4d. This is reasonable, as a larger margin would allow more tolerance for alignment errors, thereby degrading model performance.

4.7 Runtime Comparison

Lastly, we compare the overall training time of UPL-EA with three representative EA models, CPL-OT, RDGCN and RNM, across five across-lingual datasets with 30% prior seed alignments. For a fair comparison, we use the same parameters reported in the original papers of the three baselines. Fig. 5 reports the overall training time of UPL-EA and the other baselines. Our results show that UPL-EA is considerably more efficient than the three baselines, achieving a speedup of at least 50% across all five datasets.

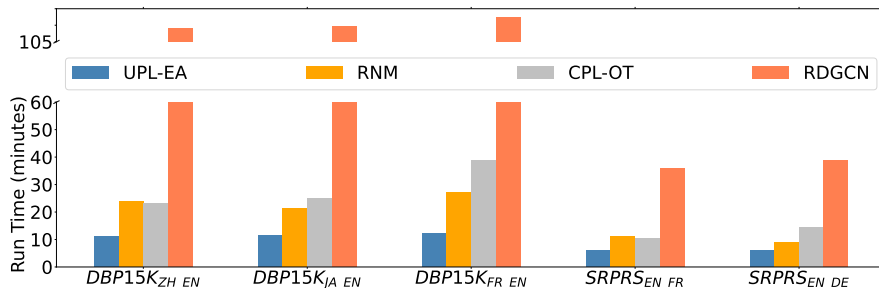


Fig. 5: Runtime comparison

Notably, CPL-OT and RNM take twice as long as UPL-EA, and three times as long in larger datasets such as DBP15K_{FR_EN}. Additionally, the supervised model RDGCN requires over 60-minute training time on DBP15K and over 30 minutes on SRPRS, indicating its poor runtime efficiency. Overall, our findings suggest that UPL-EA exhibits superior runtime efficiency compared to strong baselines.

5 Related Works

In this section, we review three streams of related literature, including entity alignment in knowledge graphs, pseudo-labeling in semi-supervised learning, and optimal transport on graphs.

5.1 Entity Alignment in Knowledge Graphs

The entity alignment (EA) task aims to discover one-to-one equivalent entity pairs across two KGs that refer to the same real-world identity. Early EA models are probabilistic methods that compute similarities and perform equivalence reasoning in the input space. For example, PARIS (Suchanek et al, 2011) is an unsupervised ontology

alignment model that matches entities, relations and entity classes to estimate the likelihood of two entities being equivalent. It is later extended to a semi-supervised EA model, PARIS+ (Leone et al, 2022), allowing the incorporation of prior seed alignments.

Since 2017, most EA models are embedding-based, using distances between entity embeddings in latent spaces to measure the semantic correspondences between entities. Inspired by TransE (Bordes et al, 2013), MTransE (Chen et al, 2017) embeds two KGs into two respective embedding spaces, where a transformation matrix is learned using prior seed alignments. To obtain better KG embeddings, TransEdge (Sun et al, 2019) enhances the translational scoring function by replacing the relation embedding with an edge embedding that incorporates information from both the head and tail entities, in addition to the relation information. To reduce the number of parameters involved, most subsequent models (Sun et al, 2017, 2018; Zhu et al, 2017) embed KGs into a common latent space by imposing the embeddings of pre-aligned entities to be as close as possible. This ensures that alignment similarities between entities can be directly measured via their embeddings.

More recent EA models leverage GNNs to incorporate KG structural information for entity alignment. For example, GCN-Align (Wang et al, 2018) adopts GCNs to learn better entity embeddings for alignment inference. However, GCNs and their variants are inclined to result in alignment conflicts, as their feature aggregation scheme incurs an over-smoothing issue (Min et al, 2020; Jiang et al, 2022): The embeddings of entities among local neighborhood become indistinguishable similar as the number of GCN layers increases. To mitigate the over-smoothing effect, more recent works (Wu et al, 2019b,a; Zhu et al, 2021) adopt a highway strategy (Srivastava et al, 2015) on GCN layers, which “mixes” the learned entity embeddings with the original features. Another line of research efforts is devoted to improving GCN-based approaches through considering heterogeneous relations in KGs. HGCN (Wu et al, 2019b) jointly learns the embeddings of entities and relations, without considering the directions of relations. RDGCN (Wu et al, 2019a) performs embedding learning on a dual relation graph, but fails to incorporate statistical information of neighboring relations of an entity. RNM (Zhu et al, 2021) uses iterative relational neighborhood matching to refine finalized entity embedding distances. This matching mechanism proves to be empirically effective, but it is used only after the completion of model training and fails to reinforce embedding learning in turn. BERT-INT (Tang et al, 2021) leverages the BERT (Bidirectional Encoder Representations from Transformers) model to capture both entity and contextual information from relational paths between entities, thereby enhancing entity alignment performance by incorporating rich semantics such as entity descriptions. Yet, obtaining powerful description information in practice can be challenging in many real-world scenarios. All the aforementioned models, however, require an abundance of prior seed alignments provided for training purposes, which are labor-intensive and costly to acquire in real-world KGs.

To tackle the shortage of prior seed alignments, semi-supervised EA models have been proposed in recent years. As a prominent learning paradigm among such, pseudo-labeling-based methods, e.g., BootEA (Sun et al, 2018), IPTransE (Zhu et al, 2017), TransEdge (Sun et al, 2019), RNM (Zhu et al, 2021), MRAEA (Mao et al, 2020), and

CPL-OT (Ding et al, 2022), propose to iteratively pseudo-label unaligned entity pairs and add them to prior seed alignments for subsequent model retraining. For RNM, there is a slight difference that it augments prior seed alignments to rectify embedding distance after the completion of model training. Although these methods have achieved promising performance gains, the confirmation bias associated with iterative pseudo-labeling has been largely under-explored. Recent methods like RNM (Zhu et al, 2021) and MRAEA (Mao et al, 2020) use simple heuristics to preserve only the most convincing alignment pairs, for example, those with the smallest distance, at the presence of conflicts. BootEA (Sun et al, 2018) and CPL-OT (Ding et al, 2022), on the other hand, model the inference of pseudo-labeled alignments as an assignment problem, where the most likely aligned pairs are selected at each pseudo-labeling iteration. Unlike BootEA that selects a small set of pseudo-labeled alignments using a pre-specified threshold, CPL-OT imposes a full match between two unaligned entity sets to maximize the number of pseudo-labeled alignments at each iteration. Both methods impose constraints to enforce hard alignments to alleviate alignment conflicts, which may potentially increase one-to-one misalignments.

This work is thus proposed to explicitly address confirmation bias in pseudo-labeling-based entity alignment. We analytically identify two types of pseudo-labeling errors that lead to confirmation bias and propose a new UPL-EA framework to alleviate these errors. Different from our previous work CPL-OT (Ding et al, 2022), UPL-EA introduces a discrete OT formulation aimed at addressing Type I pseudo-labeling errors. This formulation allows for a more accurate, probabilistic alignment configuration optimized efficiently using the Sinkhorn algorithm. Unlike CPL-OT, which relies on a pre-specified threshold, the threshold for selecting pseudo-labeled alignments in UPL-EA is mathematically derived and proven empirically effective, facilitating its applicability across various datasets. In addition, a self-ensembling approach is further proposed to refine pseudo-labeled alignments by combining predictions over multiple pseudo-labeling iterations, thus mitigating Type II pseudo-labeling errors.

5.2 Pseudo-Labeling

Pseudo-labeling has emerged as an effective semi-supervised approach in addressing the challenge of label scarcity. It refers to a self-training paradigm where the model is iteratively bootstrapped with additional labeled data based on its own predictions. The pseudo-labels generated from model predictions can be defined as hard (one-hot distribution) or soft (continuous distribution) labels (Lee, 2013; Shi et al, 2018; Arazo et al, 2020). More specifically, pseudo-labeling strategies are designed to select high-confidence unlabeled data by either directly taking the model’s predictions, or sharpening the predicted probability distribution. It is closely related to entropy regularization (Sajjadi et al, 2016), where the model’s predictions are encouraged to have low entropy (i.e., high-confidence) on unlabeled data. The selected pseudo-labeleds are then used to augment the training set and to fine-tune the model initially trained on the given labels. This training regime is also extended to an explicit teacher-student configuration (Pham et al, 2021), where a teacher network generates pseudo-labeleds from unlabeled data, which are used to train a student network.

Despite its promising results, pseudo-labeling is inevitably susceptible to erroneous pseudo-labels, thus suffering from confirmation bias (Arazo et al, 2020; Rizve et al, 2021), where the prediction errors would accumulate and degrade model performance. The confirmation bias has been recently studied in the field of computer vision. In works like (Arazo et al, 2020; Rizve et al, 2021), confirmation bias is considered as a problem of poor network calibration, where the network is overfitted towards erroneous pseudo-labels. To alleviate confirmation bias, pseudo-labeling approaches have adopted strategies such as mixup augmentation (Arazo et al, 2020) and uncertainty weighting (Rizve et al, 2021). Subsequent works like (Cascante-Bonilla et al, 2021; Zhang et al, 2021) address confirmation bias by applying curriculum learning principles, where the decision threshold is adaptively adjusted during the training process and model parameters are re-initialized after each iteration.

Recently, pseudo-labeling has also been studied on graphs for the task of semi-supervised node classification (Li et al, 2018; Sun et al, 2020a; Li et al, 2023). Li et al (2018) propose a self-trained GCN that enlarges the training set by assigning a pseudo-label to high-confidence unlabeled nodes, and then re-trains the model using both genuine labels and pseudo-labels. The pseudo-labels are generated via a random walk model in a co-training manner. Sun et al (2020a) show that a shallow GCN is ineffective in propagating label information under few-label settings, and employ a multi-stage self-training approach that relies on a deep clustering model to assign pseudo-labels. Li et al (2023) propose to incorporate the node informativeness scores for the selection of pseudo-labels and adopt distinct loss functions for genuine labels and pseudo-labels during model training. Despite these research efforts, the problem of confirmation bias remains under-explored in graph domains. This work systematically analyzes the cause of confirmation bias and proposes a principled approach to conquer confirmation bias for pseudo-labeling-based entity alignment across KGs.

5.3 Optimal Transport on Graphs

Optimal Transport (OT) is the general problem of finding an optimal plan to move one distribution of mass to another with the minimal cost (Villani, 2009). As an effective metric to define the distance between probability distributions, OT has been applied in computer vision and natural language processing over a range of tasks including machine translation, text summarization, and image captioning (Torres et al, 2021; Chen et al, 2020). In recent years, OT has also been studied on graphs to match graphs with similar structures or align nodes/entities across graphs. For graph partitioning and matching, the transport on the edges across graphs is used to define the Gromov-Wasserstein (GW) discrepancy (Titouan et al, 2019) that measures how edges in a graph compare to those in another graph (Xu et al, 2019b; Maretic et al, 2019; Xu et al, 2019a). For entity alignment across graphs, Pei et al (2019) incorporate an OT objective into the overall loss to enhance the learning of entity embeddings. Tang et al (2023) propose to jointly perform structure learning and OT alignment through minimizing multi-view GW distance matrices between two attributed graphs. These methods have primarily used OT to define a learning objective, which involves bi-level optimization for model training. To further enhance the scalability of OT modeling for entity alignment, Mao et al (2022) propose to make the similarity matrix sparse

by dropping its entries close to zero. However, this sparse OT modeling potentially violates the constraints of the OT objective, failing to guarantee one-to-one correspondences across two KGs. In our work, we focus on tackling the scarcity of prior seed alignments via iterative pseudo-labeling; we seek to find more accurate one-to-one alignment configurations between entities via OT modeling, thus eliminating conflicted misalignments at each pseudo-labeling iteration and mitigating confirmation bias.

6 Conclusion and Future Work

We have investigated the problem of confirmation bias for pseudo-labeling-based entity alignment, which has been largely overlooked in the literature. Through an in-depth analysis, we have revealed the underlying causes of confirmation bias and proposed a novel unified pseudo-labeling framework (UPL-EA) for entity alignment. UPL-EA systematically addresses confirmation bias through two key innovations: OT-based pseudo-labeling and pseudo-label ensembling. OT-based pseudo-labeling utilizes a discrete OT formulation to more accurately infer pseudo-labeled alignments that satisfy one-to-one correspondences, thus mitigating Type I pseudo-labeling errors within each iteration. Pseudo-label ensembling uses a self-ensembling approach that combines the predictions of pseudo-labeled alignments over multiple pseudo-labeling iterations to reduce pseudo-label selection variability, thus alleviating the propagation of Type II pseudo-labeling errors into subsequent model training. Our extensive experimental evaluation and analysis demonstrate that UPL-EA outperforms state-of-the-art baselines across various types of benchmark datasets. The competitive performance of UPL-EA validates its superiority in addressing confirmation bias and its utility as a general pseudo-labeling framework to improve entity alignment performance. Future research will include a theoretical investigation to rigorously assess the effectiveness of pseudo-labeling ensembling within UPL-EA. Additionally, we will explore extending our OT formulation to incorporate different sources of information for multi-modal entity alignment.

Compliance with Ethical Standards

The authors have no conflict of interests or competing interests to declare that are relevant to the content of this article.

References

- Arazo E, Ortego D, Albert P, et al (2020) Pseudo-labeling and confirmation bias in deep semi-supervised learning. In: IJCNN, IEEE, pp 1–8
- Auer S, Bizer C, Kobilarov G, et al (2007) Dbpedia: A nucleus for a web of open data. In: ISWC, Springer, pp 722–735
- Bollacker K, Evans C, Paritosh P, et al (2008) Freebase: a collaboratively created graph database for structuring human knowledge. In: SIGMOD, pp 1247–1250

- Bordes A, Usunier N, Garcia-Durán A, et al (2013) Translating embeddings for modeling multi-relational data. In: *NeurIPS*, pp 2787–2795
- Cascante-Bonilla P, Tan F, Qi Y, et al (2021) Curriculum labeling: Revisiting pseudo-labeling for semi-supervised learning. In: *AAAI*, pp 6912–6920
- Chen L, Gan Z, Cheng Y, et al (2020) Graph optimal transport for cross-domain alignment. In: *ICML*, pp 1542–1553
- Chen M, Tian Y, Yang M, et al (2017) Multilingual knowledge graph embeddings for cross-lingual knowledge alignment. In: *IJCAI*, pp 1511–1517
- Cuturi M (2013) Sinkhorn distances: Lightspeed computation of optimal transport. In: *NeurIPS*, pp 2292–2300
- Devlin J, Chang M, Lee K, et al (2019) BERT: pre-training of deep bidirectional transformers for language understanding. In: *NAACL-HLT, ACL*, pp 4171–4186
- Ding Q, Zhang D, Yin J (2022) Conflict-aware pseudo labeling via optimal transport for entity alignment. In: *ICDM, IEEE*, pp 915–920
- Guo L, Sun Z, Hu W (2019) Learning to exploit long-term relational dependencies in knowledge graphs. In: *ICML*, pp 2505–2514
- Guo Q, Zhuang F, Qin C, et al (2022) A survey on knowledge graph-based recommender systems. *IEEE Transactions on Knowledge and Data Engineering* 34(8):3549–3568
- Jiang X, Yang Z, Wen P, et al (2022) A sparse-motif ensemble graph convolutional network against over-smoothing. In: *IJCAI*, pp 2094–2100
- Laine S, Aila T (2017) Temporal ensembling for semi-supervised learning. In: *ICLR*
- Lee DH (2013) Pseudo-label: The simple and efficient semi-supervised learning method for deep neural networks. In: *ICML Workshop: Challenges in Representation Learning*, p 896
- Leone M, Huber S, Arora A, et al (2022) A critical re-evaluation of neural methods for entity alignment. *Proceedings of the VLDB Endowment* 15(8):1712–1725
- Li Q, Han Z, Wu X (2018) Deeper insights into graph convolutional networks for semi-supervised learning. In: *AAAI*, pp 3538–3545
- Li Y, Yin J, Chen L (2023) Informative pseudo-labeling for graph neural networks with few labels. *Data Mining and Knowledge Discovery* 37:228—254
- Liu X, Hong H, Wang X, et al (2022) Selfkg: Self-supervised entity alignment in knowledge graphs. In: *WWW*, pp 860–870

- Mao X, Wang W, Xu H, et al (2020) Mraea: an efficient and robust entity alignment approach for cross-lingual knowledge graph. In: WSDM, pp 420–428
- Mao X, Wang W, Wu Y, et al (2022) Lightea: A scalable, robust, and interpretable entity alignment framework via three-view label propagation. In: EMNLP, pp 825–838
- Maretic HP, Gheche ME, Chierchia G, et al (2019) GOT: an optimal transport framework for graph comparison. In: NeurIPS, pp 13876–13887
- Min Y, Wenkel F, Wolf G (2020) Scattering gcn: Overcoming oversmoothness in graph convolutional networks. NeurIPS 33:14498–14508
- Motschenbacher H (2022) Linguistic barriers in foreign language education. In: Research Questions in Language Education and Applied Linguistics: A Reference Guide. Springer, p 711–716
- Orlin JB (1997) A polynomial time primal network simplex algorithm for minimum cost flows. Mathematical Programming 78:109–129
- Paulheim H (2017) Knowledge graph refinement: A survey of approaches and evaluation methods. Semantic Web 8(3):489–508
- Pei S, Yu L, Zhang X (2019) Improving cross-lingual entity alignment via optimal transport. IJCAI, pp 3231–3237
- Pennington J, Socher R, Manning CD (2014) Glove: Global vectors for word representation. In: EMNLP, pp 1532–1543
- Pham H, Xie Q, Dai Z, et al (2021) Meta pseudo labels. In: CVPR, pp 11557–11568
- Raunak V, Gupta V, Metze F (2019) Effective dimensionality reduction for word embeddings. In: The 4th Workshop on Representation Learning for NLP, pp 235–243
- Rizve MN, Duarte K, Rawat YS, et al (2021) In defense of pseudo-labeling: An uncertainty-aware pseudo-label selection framework for semi-supervised learning. In: ICLR
- Sajjadi M, Javanmardi M, Tasdizen T (2016) Mutual exclusivity loss for semi-supervised deep learning. In: ICIP, pp 1908–1912
- Shi W, Gong Y, Ding C, et al (2018) Transductive semi-supervised deep learning using min-max features. In: ECCV 2018, pp 311–327
- Srivastava RK, Greff K, Schmidhuber J (2015) Highway networks. In: ICML Workshop: Deep Learning

- Suchanek FM, Kasneci G, Weikum G (2007) Yago: a core of semantic knowledge. In: WWW, pp 697–706
- Suchanek FM, Abiteboul S, Senellart P (2011) Paris: Probabilistic alignment of relations, instances, and schema. *Proceedings of the VLDB Endowment* 5(3)
- Sun K, Zhu Z, Lin Z (2020a) Multi-stage self-supervised learning for graph convolutional networks. In: AAAI, pp 5892–5899
- Sun Z, Hu W, Li C (2017) Cross-lingual entity alignment via joint attribute-preserving embedding. In: ISWC, pp 628–644
- Sun Z, Hu W, Zhang Q, et al (2018) Bootstrapping entity alignment with knowledge graph embedding. In: IJCAI, pp 4396–4402
- Sun Z, Huang J, Hu W, et al (2019) Transedge: Translating relation-contextualized embeddings for knowledge graphs. In: ISWC, Springer, pp 612–629
- Sun Z, Zhang Q, Hu W, et al (2020b) A benchmarking study of embedding-based entity alignment for knowledge graphs. *Proceedings of the VLDB Endowment* 13(12)
- Tang J, Zhang W, Li J, et al (2023) Robust attributed graph alignment via joint structure learning and optimal transport. arXiv preprint arXiv:230112721
- Tang X, Zhang J, Chen B, et al (2021) Bert-int: a bert-based interaction model for knowledge graph alignment. In: IJCAI, pp 3174–3180
- Tarvainen A, Valpola H (2017) Mean teachers are better role models: Weight-averaged consistency targets improve semi-supervised deep learning results. In: NeurIPS, pp 1195–1204
- Titouan V, Courty N, Tavenard R, et al (2019) Optimal transport for structured data with application on graphs. In: ICML, pp 6275–6284
- Torres LC, Pereira LM, Amini MH (2021) A survey on optimal transport for machine learning: Theory and applications. arXiv preprint arXiv:210601963
- Villani C (2009) *Optimal transport: old and new*, vol 338. Springer
- Vrandečić D, Krötzsch M (2014) Wikidata: a free collaborative knowledge base. *Communications of the ACM* 57(10):78–85
- Wächter A, Biegler LT (2006) On the implementation of an interior-point filter line-search algorithm for large-scale nonlinear programming. *Mathematical Programming* 106:25–57
- Wang Z, Zhang J, Feng J, et al (2014) Knowledge graph embedding by translating on hyperplanes. In: AAAI, pp 1112–1119

- Wang Z, Lv Q, Lan X, et al (2018) Cross-lingual knowledge graph alignment via graph convolutional networks. In: EMNLP, pp 349–357
- Wu Y, Liu X, Feng Y, et al (2019a) Relation-aware entity alignment for heterogeneous knowledge graphs. In: IJCAI, pp 5278–5284
- Wu Y, Liu X, Feng Y, et al (2019b) Jointly learning entity and relation representations for entity alignment. In: EMNLP/IJCNLP, pp 240–249
- Xu H, Luo D, Carin L (2019a) Scalable gromov-wasserstein learning for graph partitioning and matching. In: NeurIPS, pp 3046–3056
- Xu H, Luo D, Zha H, et al (2019b) Gromov-wasserstein learning for graph matching and node embedding. In: ICML, pp 6932–6941
- Yang H, Zou Y, Shi P, et al (2019) Aligning cross-lingual entities with multi-aspect information. In: EMNLP/IJCNLP, pp 4430–4440
- Yang Z, Qi P, Zhang S, et al (2018) Hotpotqa: A dataset for diverse, explainable multi-hop question answering. In: EMNLP, pp 2369–2380
- Zeng W, Zhao X, Tang J, et al (2020) Collective entity alignment via adaptive features. In: ICDE, IEEE, pp 1870–1873
- Zhang B, Wang Y, Hou W, et al (2021) Flexmatch: Boosting semi-supervised learning with curriculum pseudo labeling. In: NeurIPS, pp 18408–18419
- Zhao X, Zeng W, Tang J, et al (2020) An experimental study of state-of-the-art entity alignment approaches. *IEEE Transactions on Knowledge and Data Engineering* 34(6):2610–2625
- Zhu H, Xie R, Liu Z, et al (2017) Iterative entity alignment via knowledge embeddings. In: IJCAI, pp 4258–4264
- Zhu Y, Liu H, Wu Z, et al (2021) Relation-aware neighborhood matching model for entity alignment. In: AACL, pp 4749–4756